A review of geometry optimisation of wave energy converters

Citation for published version:
Garcia Teruel, A & Forehand, D 2021, 'A review of geometry optimisation of wave energy converters', *Renewable and Sustainable Energy Reviews*, vol. 139, 110593. https://doi.org/10.1016/j.rser.2020.110593

Digital Object Identifier (DOI):
10.1016/j.rser.2020.110593

Published In:
Renewable and Sustainable Energy Reviews

A review of geometry optimisation of wave energy converters

Garcia-Teruel, A.[a,*], Forehand, D.I.M.[a]

[a] *Institute for Energy Systems, School of Engineering, The University of Edinburgh, Edinburgh, United Kingdom EH9 3BF*

Abstract

Reducing the cost of energy of wave energy converters is key for the advancement of the technology. The costs associated with the device structure show the highest potential to achieve this reduction. For this reason, many hull geometry optimisation studies have been performed over the last 20 years, with the aim of finding improved hull shapes, that maximise the power generation and minimise the costs. These studies have been performed for different types of devices, applying a number of optimisation algorithms and representing power generation and costs with various strategies. The definition of the optimisation problem and the use of the most suitable strategies is key for a successful optimisation process, which will provide meaningful results and support device design at early development stages. This paper reviews all these different approaches, with a view to distilling the main findings and best practices; it then formulates recommendations based on these. The work is intended to serve as reference for any technology developer wishing to perform wave energy converter optimisation and for any funding body wanting to assess different device designs.

Highlights

- Wave energy converter hull optimisation results can be significantly improved through the use of flexible geometry definitions, such as using B-spline functions.
- The choice of optimisation algorithm and set-up should be used to

*Corresponding author
Email address: a.garcia-teruel@ed.ac.uk (Garcia-Teruel, A.)

improve computational time without reducing model accuracy.

- Annual energy production and surface area based objective functions generate the overall most consistent and realistic shapes and performance results.

Keywords: Optimisation problem, Hull geometry, Wave energy converter, Device design, Cost of energy
Wordcount=9525 words

Nomenclature	**Definition**	**Unit**
B	Characteristic length of a device	m
f	Objective function	NA
g	Gravitational acceleration	m/s^2
$\mathbf{g}$	Set of equality constraints	NA
$\mathbf{h}$	Set of inequality constraints	NA
H_{m0}	Significant wave height	m
n	Design lifetime	years
$O(H_{m0}, T_z)$	Percentage occurrence of a sea state	%
P_{proxy}	Nomenclature used to indicate metric employing power performance in combination with cost proxy	NA
$\bar{P}(H_{m0}, T_z)$	Mean power per sea state	W
$\bar{P}_{overall}$	Overall mean power	W
$\bar{P}_{pm}$	Power per metre crest width	W/m
$\bar{P}_q(t)$	Instantaneous available power from the PTO	W
r	Discount rate	[%]
T_e	Energy period	s
T_z	Zero-crossing wave period	s
$\mathbf{C}$	Damping matrix	kg/s, (kg m)/s, and (kg m^2)/s
$\mathbf{F}$	Force vector	N and Nm
$\mathbf{K}$	Stifness matrix	kg/s^2, (kg m)/s^2, and (kg m^2)/s^2
$\mathbf{M}$	Mass matrix	kg, kg m, and kg m^2
$\mathbf{x}$	Vector of decision variables	NA
$\mathbf{X}$	Fourier transform of the position vector $\mathbf{x}(t)$	m
$\dot{\mathbf{X}}$	Fourier transform of the velocity vector $\dot{\mathbf{x}}(t)$	m/s
$\ddot{\mathbf{X}}$	Fourier transform of the acceleration vector $\ddot{\mathbf{x}}(\mathrm{t})$	m/s^2
ρ	Water density	kg/m^3
ω	Wave frequency	rad/s
Ω	Solution Space	NA

Nomenclature	Definition	Unit
AEP	Annual Energy Production	MWh
BEM	Boundary Element Method	NA
CapEx	Capital Expenditures	€
COBYLA	Constrained Optimisation BY Linear Approximation’	NA
CW	Capture Width	m
CWR	Capture Width Ratio	%
FEM	Finite Element Method	NA
GA	Genetic Algorithm	NA
LCOE	Levelised Cost Of Energy	€/MWh
NPV	Net Present Value	NA
OpEx	Operational Expenditures	€
PTO	Power Take-Off	NA
RAO	Response Amplitude Operator	-
RMS	Root Mean Square	NA
RSM	Response Surface Method	NA
TPL	Technology Performance Level	-
TRL	Technology Readiness Level	-
WEC	Wave Energy Converter	NA

1. Introduction

Many different Wave Energy Converter (WEC) concepts have been developed in the past years, with the goal of finding an economically competitive design, which at the same time enables maximal power extraction. One of the biggest cost reduction potentials has been associated with the device structure. In a report from Sandia National Laboratories [1], optimised structural design, and device size and shape were identified as two of the four most promising pathways for cost reduction in the development of WECs. This agrees with the SI OCEAN report [2], which identifies the structure and prime mover to account for up to 31% of the average WEC lifetime costs. Other techno-economic assessment studies classify the prime mover structure as the biggest cost center, accounting, for example, for 28% of the manufacturing costs in [3], and 32% of the Levelised Cost Of Energy (LCOE) in [4]. In the former study, the structural cost is represented by the price per kilogram of material and the volume of the device. In the latter, it is represented through a characteristic dimension of the device and the percentage of LCOE of the prime mover costs. Already in 1996, French [5] had identified three main measures for systematic WEC design[1] which reflected the relevance of the working surface area and the submerged volume, both defined by the WEC hull geometry. More recently, the potential for economical benefit has also been found in the optimisation of the interaction between WEC geometry and control strategy [6].

The fact that high cost reduction potential has been associated with the device's structure, and the existing lack of consensus in the device design; has revealed the need for inclusion of geometry optimisation studies to help determine the device's shape in the early stages of the design process. As a result, many varied geometry studies have been performed in the past years for different types of devices. These will be reviewed in this paper, with a view to distilling the most successful approaches and best practices.

With this goal in mind, geometry and optimisation studies for other offshore applications are reviewed (section 2), the main characteristics of WEC geometry optimisation are identified and characterised (section 3), and the reviewed literature is sorted according to the identified characteristics (section 4). Finally, recommendations for future geometry optimisation studies based on the existing results are given (section 5 and 6).

2. Geometry studies in offshore applications

Geometry and optimisation studies have been performed in the past, not only for WEC devices, but also for other offshore applications, which have served as example and inspiration for some of the WEC geometry studies. A reduced sample of these studies is reviewed here to give an overview of common practices in related fields.

2.1. Design of ship hulls and offshore structures

Ship hull design and optimisation has been applied and developed for a number of decades, and many different aspects have been investigated [7]. Clauss and Birk [8] optimised the shape of large offshore structures to improve

[1]The three measures include: 1) area ratio = area of working surface/total area of surface, 2) amplitude ratio = amplitude of working surface/amplitude of wave and 3) swept volume ratio = (0.5 × volume swept by working surface)/(total area of surface × wave amplitude)

their seakeeping capabilities by introducing a so called 'significant double amplitude of overturning moment'. This is calculated from a response spectrum corresponding to the wave spectrum and a significant force, in an analogous manner to how the significant wave height is obtained from the wave spectrum. This significant double amplitude was then used as the objective function in an optimisation process to generate improved offshore structures with reduced oscillatory motions. This method was applied to gravity base structures, tension leg platforms and semisubmersibles, achieving a decrease in overturning moment of up to 89% for a caisson semisubmersible. Later, Birk [9] applied Genetic Algorithms (GAs) to geometry optimisation of offshore structure hulls. In that study, payload is maximised and downtime (represented by the significant double amplitude exceeding operational requirements limits) is minimised. The resulting optimal shapes show downtime values between 9 and 11% and displacement to payload ratios between 5.7 and 6.5.

Manufacturability has been considered for ship hull design for many years, where rolled mild steel sheets are the most widely used. Composite materials have also been used for bulkheads and moulded hulls, where Glass Reinforced Plastics (GRP) were used in 95% of these cases [10]. In [11], Letcher gives an overview of ways of defining hull geometries using B-spline surfaces, among other methods, and recommends the use of developable surfaces in hull design for ease of manufacturing. How to use developable surfaces in hull design was first described by Kilgore in [12] and has since been widely used for ship hull fabrication [11]. Methods to ensure the smoothness of the surfaces for aesthetic and manufacturing ease purposes have also been developed, as reported in [13]. Most recent studies have then further investigated the above concepts for their use in the Computer Aided Design and optimisation processes [14, 15, 16, 17].

2.2. Wave energy converter design

Optimisation has been used in WEC design not only for finding suitable hull shapes, but also for the design of other components such as the Power Take-Off (PTO) system, or the mooring lines. An example of a PTO-system optimisation was given by Nambiar et al. [18], where the optimal dimensions of a hydraulic PTO-system (diameter of hydraulic piston, volume of the hydraulic accumulators and motors, and generator speed) were studied with help of a wave-to-wire model. Extensive work has been undertaken in control system optimisation for WECs, where optimisation has been used in two contexts: to design the control strategy, for example, to determine single parameters such as the damping and stiffness of the PTO; or during the control application to determine the output signal based on the input information, such as in model predictive control. A very good overview of different control strategies and of these two sides of optimisation within a controls' context can be found in [19]. Optimisation studies for mooring lines have not been done so extensively, however, some studies exist which optimise mooring design to maximise power [20] or minimise costs [21]. Analysing mooring dynamics is computationally expensive and, for this reason, surrogate optimisation methods were used in these studies. Another large field of study, where optimisation has been employed, is array layout optimisation. Some examples of these studies are [22, 23, 24]. A preliminary study on the effect of device size within the array layout has been presented in [25]. De Andres also analysed the economically more suitable solutions for WECs regarding optimal device size, in terms of rating and number of WECs within an array, for a specific location [26].

In summary, the application of optimisation to WEC design has been extensive. The present review concentrates on hull shape optimisation studies, due to the increased number of these types of studies in recent years, which were motivated by the high potential for cost reduction associated to the device structure.

3. Key elements of a geometry optimisation process

For a systematic analysis of the different geometry optimisation studies, the key elements that describe such a process are identified. These elements are introduced in detail in each of the subsections in order to provide a common basis of terminology and understanding to compare the different studies. To begin with, the general definition and formulation of an optimisation process are introduced.

In a single-objective optimisation process, the solution $\mathbf{x}$ that minimises an objective function $f(\mathbf{x})$, while fulfilling a set of equality constraints $\mathbf{g}$ and inequality constraints $\mathbf{h}$, is sought.[2] Single-objective optimisation problems

[2]Normally optimisation processes are set up for minimisation problems. Maximisation problems can just be rearranged into minimisation problems.

can, therefore, be formulated as follows in the standard form [27]:

$$
\begin{array}{ll}
\min f(\mathbf{x}) & \\
\text{objective function:} & f(\mathbf{x}) \\
\text{decision variables:} & \mathbf{x} = \{x_1, ..., x_k\} \in \Omega \\
\text{equality constraints:} & g_i(\mathbf{x}) = 0 \quad \text{for} \quad i = 1, .., m \\
\text{inequality constraints:} & h_j(\mathbf{x}) \leq 0 \quad \text{for} \quad j = 1, .., l
\end{array} \tag{1}
$$

In Multi-objective Optimisation Problems (MOPs), optimal solutions for problems with various conflicting objectives $(f_1, f_2, ..., f_n)$ are sought. As opposed to the single-objective optimisation problems, not only one but multiple solutions will be optimal depending on the importance or weight of each objective function. The set of optimal solutions is represented through a so called Pareto Front.

$$
\begin{array}{ll}
\min \mathbf{f}(\mathbf{x}) & \\
\text{objective functions:} & \mathbf{f}(\mathbf{x}) = \{f_1, f_2, ..., f_n\} \\
\text{decision variables:} & \mathbf{x} = \{x_1, ..., x_k\} \in \Omega \\
\text{equality constraints:} & g_i(\mathbf{x}) = 0 \quad \text{for} \quad i = 1, .., m \\
\text{inequality constraints:} & h_j(\mathbf{x}) \leq 0 \quad \text{for} \quad j = 1, .., l
\end{array} \tag{2}
$$

A solution $\mathbf{x}$ is feasible, if it fulfills all constraints $\mathbf{g}$ and $\mathbf{h}$, while respecting the decision variable bounds. Decision variable bounds define the limits of the solution space Ω. General concepts for single and multi-objective optimisation are explained in the literature [28, 29, 30].

How objective functions, constraints and decision variables need to be defined in a WEC geometry optimisation process is explained based on the general flow diagram represented in Figure 1.

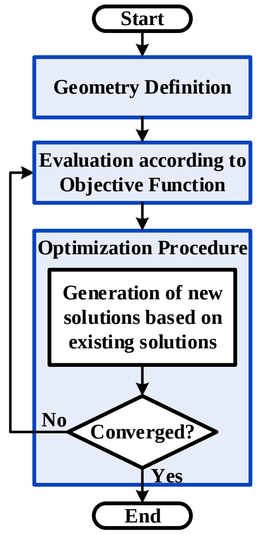

Figure 1: Representation of a WEC geometry optimisation process.

From this diagram, the following key elements that will characterise such a process can be identified:

- WEC type - The choice of WEC technology to be studied can highly influence all the other elements.
- Geometry definition - How the starting geometry and decision variables are defined will influence the range of possible solutions, e.g. if a cylinder is used as the starting shape and its diameter and draft are chosen as the decision variables, only cylinders of variable size can be solutions of the optimisation process.
- Objective function - Depending on the metrics used as objective functions; and the models, and assumptions used to calculate these metrics, certain solutions will be favoured over others.
- Optimisation procedure - The choice of the optimisation algorithm for each application will, firstly have an influence on the required computational time, depending on the algorithm's efficiency and this will constrain what type of evaluation can be performed; and secondly, it will affect the convergence of the process into more or less suboptimal solutions.

After identification of these key elements, each of them will be briefly described and characterised in the following sections to enable the sorting of existing studies. It should be noted that for the purpose of completeness, not only geometry optimisation studies but what we will call 'geometry comparison studies' are also reviewed here. Geometry comparison studies do not include an actual optimisation process, but compare a number of pre-defined geometries or geometry variations. Studies using some type of parametric search are also included under this definition. These two types of studies are reported separately throughout this review.

3.1. Wave energy converter types

Different WEC types have been identified based on their working principle and some examples and explanation of their respective characteristics can be found in [31, 32]. Table 1 describes some of the main types and lists some associated geometry comparison and geometry optimisation studies. Generic versions of the considered WEC types are represented in Figure 2. The structural components commonly considered for geometry optimisation are shown in grey. Given the fact that many studies exist for floating devices (categories A, B, C, E) and, in particular, point absorbers (A-C), more specific categories are considered here for these types of devices. Based on the radiation type, a differentiation can be made between point absorbers (source mode radiators) and quasi-point absorbers (dipole radiators). For the purposes of generalisation and categorisation, here both types are referred to as point absorbers. For categories not mentioned here, no geometry studies were available to the knowledge of the authors.

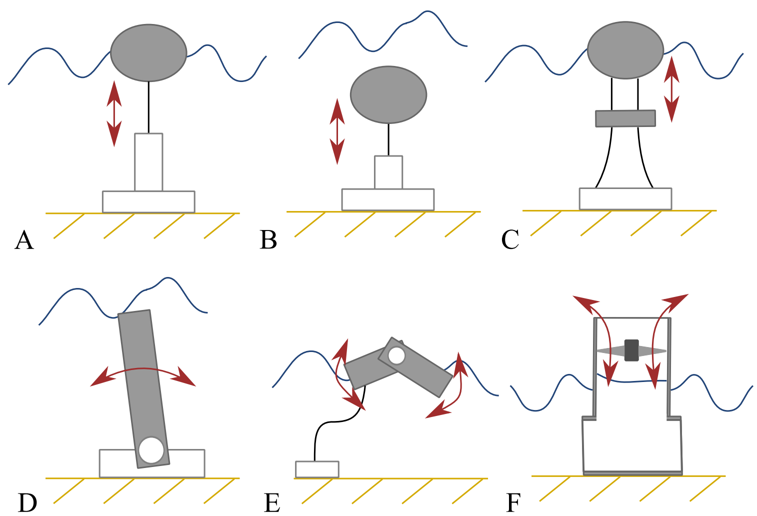

Figure 2: Representation of generic WEC types listed in Table 1. Their oscillation is indicated with red arrows. In case F, the arrows indicate the air flow through the turbine.

Table 1: Studied WEC types in geometry comparison and optimisation studies.

WEC type label	**WEC type description**	**Relevant comparison studies**	**Relevant optimisation studies**
A	point absorber - single body - floating	[33], [34], [35], [36], [37], [38], [39], [40], [41], [42], [43], [26], [44], [45], [46], [47], [48], [49], [50]	[51], [52], [53], [54], [55], [56], [57], [58], [59], [60],[61], [62], [63]
B	point absorber - single body - submerged	[64], [65], [66]	[67], [68], [69]
C	point absorber - two body	[70], [71], [72]	[73], [74], [56], [75]
D	terminator - hinged flap	[76], [77]	[78], [79], [80]
E	attenuator	[81], [82], [83]	[84], [85], [86]
F	oscillating water column	[87], [88], [89], [90]	[91], [92], [93], [94], [95], [96], [97], [98], [99]

3.2. Geometry definition

Different geometry representations have been used to perform geometry comparison and optimisation studies of WEC devices. Most studies can be categorised within the geometry definitions represented in Figure 3 and described in Table 2, although this categorisation applies mostly to floating devices. The predominant wave direction in these studies is in the positive x-direction.

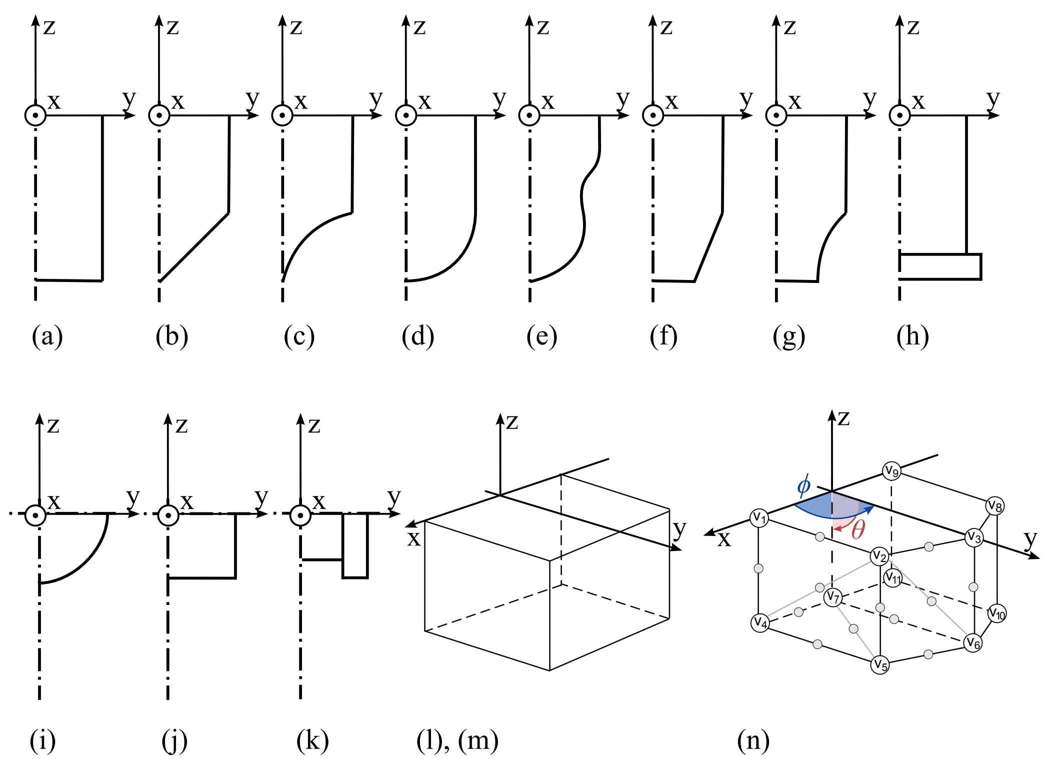

Figure 3: Overview of geometry definition options considered in the literature for WEC devices.

The most studied device representation is the vertical cylinder heaving buoy, where the chosen decision variables are usually the draft and radius, however, other relations, such as the submerged surface to draft ratio [34] have been investigated and further variables, such as the body and bottom wall thickness, have also been considered [43]. Many variations of the vertical cylinder type device have been examined (e.g. geometries (b)-(h)). The most adaptable geometry definitions, in which the optimisation results can show the largest variation in shape, were achieved in [53, 55] (i.e. geometry (n)), followed by [57] (i.e. geometry (e)). In geometry (n), bi-cubic B-spline surfaces were used to represent the submerged WEC hull and in geometry (e), polynomial and Bézier curves were used for the axisymmetric WEC shape. Following a similar idea, Fourier decomposition was used for a submerged heaving disc to parametrically represent the shape's cross-section in [69]. In [63] it was found that using adaptable geometry definitions versus standard shapes such as a sphere, a barge or a cylinder could result in an improvement in objective function values of up to 224%.

Some interesting studies have also been performed on devices of deformable shape [66] and controlled geometry [77], where the aim in the latter was to reduce the loads by varying the exposed surface area. In addition, devices of variable size were studied in [41] from a perspective of their economic suitability regarding site-specific natural frequency tuning.

Table 2: Studies using each of the geometry definitions from Figure 3.

WEC shape label	**WEC shape description**	**Relevant comparison studies**	**Relevant optimisation studies**
(a)	vertical cylinder	[34], [70], [36], [64], [38], [40], [41], [42], [43], [44], [45], [47], [49], [50], [72]	[52], [74], [56], [58]
(b)	vertical cylinder with conical bottom	[35], [70],[36], [74], [37], [45], [47], [50]	-
(c)	vertical cylinder with concave bottom	[36]	-
(d)	vertical cylinder with spherical bottom	[35], [36], [38], [45], [47], [50]	-
(e)	axisymmetric body defined by polynomial	[46]	[57]
(f)	vertical cylinder with truncated conical bottom	[38], [71], [48]	-
(g)	vertical cylinder with truncated concave bottom	[38]	-
(h)	vertical cylinder of variable inner or outer crosssection	[70]	-
(i)	sphere	[38], [37]	-
(j)	horizontal cylinder	[81], [65], [37], [82]	[67], [68],[51], [78]
(k)	horizontal cylinder of variable outer crosssection	-	[54]
(l)	barge or rectangular shape	[48], [83]	[91], [84], [51], [86]
(m)	flap	[76], [77]	[78], [79], [80]
(n)	x-z plane symmetric body defined by spline surfaces	-	[53], [55], [59], [60], [61], [63]
(o)	specific WECs	[87], [81], [88], [64], [39], [71], [26], [46], [66], [89], [72], [90]	[92, 93, 94, 95], [51],[73], [85], [96], [56], [97], [75] [62]

The final entry in Table 2 relates to studies of specific WECs, where the basic shape of the device was given and certain parameters were varied, such as with the SEAREV [51], the Columbia Power [85], and the IPS [56] devices, or a simple scaling was performed, such as with the Reference Model 3 device [75].

3.3. Objective function

In an optimisation problem, the objective function represents the characteristic that will be maximised or minimised depending on the values of the decision variables. Different metrics can be used in one objective function to represent the characteristic or the trade-off of characteristics that the designer is interested in. In geometry comparison studies, the different designs are also compared based on certain metrics depending on the purpose of the investigation.

The Levelised Cost Of Energy (LCOE) is widely used in the energy generation industry as a metric that enables comparison between different technologies, based on their generation costs. It is also used within the wave energy sector to compare different devices. The LCOE describes the ratio of Capital (CapEx) and Operational (OpEx) Expenditures to the Annual Energy Production (AEP), discounted to their Net Present Values (NPV), through a discount rate r and a design lifetime n:

$$\mathrm{LCOE} = \frac{\mathrm{NPV(CapEx + OpeEx)}}{\mathrm{NPV(AEP)}} = \frac{\sum_{t=0}^{n}(\mathrm{CapEx}_t + \mathrm{OpeEx}_t)/(1+r)^t}{\sum_{t=0}^{n}(\mathrm{AEP})/(1+r)^t} \quad (3)$$

However, given the lack of available costs information, it is difficult to use this metric at early design stages. For this reason, other methods for quantifying the trade-off between power generation and costs have been developed with the goal of allowing device comparison.

From a techno-economic perspective, metric comparison studies were performed by de Andrés et al. [100] and methods for economic assessment of WECs were reviewed by Astariz and Iglesias [101]. Yu et al. [76] have proposed a whole system economic model, however, only a few examples of models aiming at a whole system economic evaluation exist, such as that implemented by Teillant et al. [3].

From a power performance perspective, different metrics are applied to eight different types of WECs in [102]. Additionally, different Technology Readiness Levels (TRLs) have been identified at which different Technology

Performance Levels (TLPs) can be expected. In [103] an overview of the expected analysis methods and metrics used at each TRL is given.

3.3.1. Modelling methods

With the aim of introducing the various performance metrics used for WEC geometry comparison, general numerical models and their differences are specified in the following.

Assuming small harmonic oscillations, the WEC response can be calculated for single wave frequencies (ω) in the frequency-domain, and the oscillations for multiple wave frequencies can then be linearly superposed to obtain the response in irregular seas. The frequency-domain equation of motion for a WEC oscillating in six degrees-of-freedom can be written as equation (4):

$$\begin{aligned}-\omega^2\mathbf{M}\hat{\mathbf{X}} &= \hat{\mathbf{F}}_{ex} + \hat{\mathbf{F}}_H + \hat{\mathbf{F}}_{rad} + \hat{\mathbf{F}}_{PTO} + \hat{\mathbf{F}}_m + \hat{\mathbf{F}}_{loss} \\ &= \hat{\mathbf{F}}_{ex} - \mathbf{K}_H\hat{\mathbf{X}} - (-\omega^2\mathbf{M}_{rad}\hat{\mathbf{X}} + i\omega\mathbf{C}_{rad}\hat{\mathbf{X}}) \\ &- (-\omega^2\mathbf{M}_{PTO}\hat{\mathbf{X}} + i\omega\mathbf{C}_{PTO}\hat{\mathbf{X}} + \mathbf{K}_{PTO}\hat{\mathbf{X}}) + \mathbf{F}_m + \mathbf{F}_{loss},\end{aligned} \tag{4}$$

where $\mathbf{M}$ is the mass matrix and $\hat{\mathbf{X}} = \hat{\mathbf{X}}(\omega)$, $i\omega\hat{\mathbf{X}} = i\omega\hat{\mathbf{X}}(\omega)$ and $-\omega^2\hat{\mathbf{X}} = -\omega^2\hat{\mathbf{X}}(\omega)$ are the Fourier transforms of the position $\mathbf{x}(t)$, velocity $\dot{\mathbf{x}}(t)$ and acceleration $\ddot{\mathbf{x}}(t)$ of the device, respectively. $\hat{}$ indicates complex amplitude. The device oscillations are influenced by a set of forces: the wave excitation force $\hat{\mathbf{F}}_{ex}$, the hydrostatic force $\hat{\mathbf{F}}_H$, the radiation force $\hat{\mathbf{F}}_{rad}$, the PTO force $\hat{\mathbf{F}}_{PTO}$, the mooring force $\hat{\mathbf{F}}_m$ and a dissipative force representing friction losses $\hat{\mathbf{F}}_{loss}$. The hydrostatic force can be represented through a hydrostatic stiffness $\mathbf{K}_H$ based on the Archimedes principle; the radiation force is composed of an added mass $\mathbf{M}_{rad}$ and an added damping $\mathbf{C}_{rad}$ terms; and the PTO force can have a different number of components, depending on the control strategy employed. To include friction losses in a simplified manner, the dissipative force $\hat{\mathbf{F}}_{loss}$ can be represented through a damping term $\mathbf{C}_{loss}$ as in [104]. When the device oscillations are normalized by the incoming wave amplitude, they are called Response Amplitude Operator (RAO).

The mean power absorbed by the PTO over a sinusoidal wave cycle is given by :

$$\bar{P} = \frac{1}{2}\omega^2\hat{\mathbf{X}}^T\mathbf{C}_{PTO}\hat{\mathbf{X}}^*, \tag{5}$$

where $\hat{\mathbf{X}}$ is a 6×1 column vector, ^{T} indicates transposed and * the complex conjugate. The value obtained through this power calculation at the resonance period is called the maximum absorbed power. This is an indicator of the mean unconstrained power for a given sea state.

To obtain the irregular-sea response time-series of mode i from the frequency-domain analysis, the sum over all considered spectral frequency components ω_k can be taken:

$$x_{i,q}(t) = \sum_{k=1}^{N} \left(|X_i(\omega_k)| cos(\omega_k t + \psi_{k,q} + \angle X_i(\omega_k)\right); \quad q = 1,..,Q; \quad i = 1,..,6, \tag{6}$$

where $\psi_{k,q}$ are a set of random phase shifts and Q denotes the number of random realisations of the same irregular sea state. Obtaining a time-series from a frequency-domain formulation will be referred to here as pseudo time-domain model. This analysis can be performed with a certain frequency step ($\Delta\omega$) for a maximal non-repeating time series of duration $\frac{2\pi}{\Delta\omega}$. In this case, the instantaneous available power from the PTO is calculated using equation (7).

$$P_q(t) = \dot{\mathbf{x}}_q^T(t)[\mathbf{C}_{PTO}]\dot{\mathbf{x}}_q(t). \tag{7}$$

With this formulation, stroke and rated power limits can be considered, for example, by setting the instantaneous power to 0 or to its maximum, respectively, if these limits are exceeded (as in [55]), without need for a proper time-domain analysis. This means that $P_q(t)$ is only an approximation to the actual instantaneous constrained power. In some studies, the square of the velocity $\dot{\mathbf{x}}_q(t)$ is used to represent the instantaneous power, such as in [38, 40]. This is because following equation (7) the absorbed power is proportional to the velocity squared. However, as can also be seen from equation (7), using only the velocity squared to represent power does not take into account the PTO absorption capabilities and possible changes in the control strategy defined through tuning of the PTO damping coefficient (C_{PTO}).

Alternatively, to be able to account for non-linear effects, such as viscous drag, or specific PTO-control strategies, a pure time-domain formulation is required, as represented by equation (8). This formulation is based on Cummins formulation [105], which assumes that the hydrostatic and hydrodynamic forces are linear.

$$(\mathbf{M} + \mathbf{M}_{rad}(\infty))\ddot{\mathbf{x}}(t) = \mathbf{F}_{ex}(t) - \mathbf{K}_H\mathbf{x}(t) - \int_0^t \mathbf{K}_{rad}(t-\tau)\dot{\mathbf{x}}(\tau)d\tau + \mathbf{F}_{PTO}(t). \tag{8}$$

In equation (8), $\mathbf{M}_{rad}(\infty)$ is the added mass matrix at infinite frequency and $\mathbf{K}_{rad}(t)$ is the radiation impulse response function, which is the inverse Fourier transform of the radiation impedance function $C_{rad}(\omega) + i\omega(\mathbf{M}(\omega) - \mathbf{M}_{rad}(\infty))$. The radiation convolution term $\int_0^t \mathbf{K}_{rad}(t-\tau)\dot{\mathbf{x}}(\tau)d\tau$ can be computationally demanding to calculate and is often replaced by an approximating state-space model, which is obtained either by Time-Domain Identification (TDI) (e.g. Prony's method) or Frequency-Domain Identification (FDI) [106]. The instantaneous power is then calculated by inserting $\dot{\mathbf{x}}(t)$ from equation (8) into equation (7).

The overall mean annual power is obtained by summing, over all sea states (with a sea state represented by H_{m0} and T_z), the product of the percentage occurrence of a sea state $O(H_{m0}, T_z)$ and the mean power produced in that sea state $\bar{P}(H_{m0}, T_z)$ (see equation(5)). That is, the overall mean power is given by the expression below.

$$\bar{P}_{overall} = \sum_{H_{m0}} \sum_{T_z} O(H_{m0}, T_z)\bar{P}(H_{m0}, T_z), \tag{9}$$

The Annual Energy Production (AEP) is then obtained from $\bar{P}_{overall}$ by multiplying it by the number of seconds in a year. These two measures are grouped here under the term AEP for generalisation purposes.

A review of wave energy theory is provided in [107], where modelling approaches for coupled resonant systems are introduced. For the specific modelling of oscillating water columns refer to [108].

Regarding the representation of the WEC deployment site, different approaches have been used. The least computationally demanding and most simple approach is to analyse the performance of the device in regular waves with a specific period and wave height, such as in [43]. Alternatively, irregular waves can be represented by the superposition of regular waves. Different techniques have been employed to reduce the required computational time, such as: representing a sea state by a regular wave with a characteristic wave height and period that match the sea state wave energy and power obtained from an irregular wave representation [56], or by using occurrence matrices with reduced number of sea states [74, 56, 96]. Goggins et al. [38] compared the preferred shapes resulting when using the single year versus a three-year averaged scatter diagram for the AMETS site. The optimal shape for the single year and the averaged scatter diagrams was, however, the same: a hemispherical-bottomed cylinder. The sensitivity of the optimal design parameters to the use of single sea-states or a combination of three sea-states was investigated in [93]. Multidirectional waves have only been considered by Esmaelizadeh et al. in [69], where the effect of using regular and irregular, unidirectional and multidirectional waves for one sea state on optimal wave energy converter shapes was studied. Asymmetrical butterfly-like shapes were preferred when multidirectional sea conditions with an asymmetric angular distribution of the incident waves were considered. Otherwise, symmetrical shapes were selected through the optimisation.

From a hydrodynamic model point of view, the simplest approach is to use a frequency-domain method, with which PTO-stroke and power rating constraints, and viscous and non-linear forces are not considered [54]. A pseudo time-domain calculation that includes PTO-stroke and power rating constraints was used in [55]. Time-domain models allow for consideration of real PTO-systems [56], but if based on linear wave theory do not allow for consideration of extreme sea conditions. Through inclusion of an additional quadratic damping term based on Morison's equation, viscous effects can be represented, as done, for example, in [102].

3.3.2. Example metrics for geometry evaluation

Based on the above definitions and modelling methods, different relationships have been used to represent power performance:

1. Capture Width (CW) is defined as the ratio of average absorbed power $\bar{P}$ to the wave resource, represented by the power per metre crest width P_{pm}, and therefore has units of length:

$$\mathrm{CW} = \frac{\bar{P}}{P_{pm}}, \tag{10}$$

$$\text{where} \quad P_{pm} = \frac{\rho g^2 T_e H_{m0}^2}{64\pi} \quad \text{for deep water.} \tag{11}$$

   Here ρ is the water density, g the gravitational acceleration, T_e the energy period, and H_{m0} the significant wave height. CW according to equation (10) is defined for a particular sea state. To calculate CW at a particular location the CW values of a given sea state are multiplied by the corresponding sea state occurrence and added over all sea states, similarly as done to calculate the overall power in equation (9).

2. The Capture Width Ratio (CWR) is defined as CW divided by a characteristic length of the device B. What should be considered as the characteristic length for different types of devices is described in [102, 109]. Although when compared to CW, this measure takes into consideration device size in the objective function, and this avoids the optimisation from converging to very big devices, the definition of a characteristic length for different types of devices is not straightforward. The CWR for a particular location rather than for a single sea state is calculated as described for CW.

$$\text{CWR} = \frac{\bar{P}}{P_{pm}B} \tag{12}$$

3. For two-dimensional problems (e.g. devices in a flume, a terminator that is infinitely long, or an infinitely long row of devices aligned perpendicular to the wave direction), a measure of efficiency η based on the far-field radiation can be used [110], [33], [39]. If the device oscillates in a single mode i, equation (13) applies, where the ratio of the radiated wave amplitude upstream (A_i^-) and downstream of the device (A_i^+) is employed. This is based on the understanding that if the radiated wave amplitude downstream of the device is zero, and waves are radiated upstream of the device, the efficiency would be 1. If the device is symmetric front-to-back the maximum efficiency would be 0.5. In this case, $0 \leq \eta \leq 1$. For devices oscillating in multiple modes of motion, the general form defined by Falnes in [111] applies.

$$\eta = \frac{1}{1+\gamma^2} \quad \text{with} \quad \gamma = \left| \frac{A_i^+}{A_i^-} \right|. \tag{13}$$

To account for costs in the objective function, various cost proxies, such as mass, volume or surface area, etc., have been used. Studies which use similar proxies have been grouped together and labelled by the symbol P_{proxy}. Here P can stand for the absorbed energy [Wh] or power [W] and studies in the P_{proxy} group either use $\frac{P}{proxy}$ for the objective function or, in the case of multiobjective optimisation, they could use P and $proxy$ individually, or multiple ratios simultaneously. The proxies that have been considered are:

1. Mass (i.e. the group P_m), where the characteristic [102, 76], or the displaced mass [51, 57] have been employed.

2. Volume (i.e. the group P_V), where the total [43] or the submerged volume [55, 74, 73, 56] have been used.
3. Surface area (i.e. the group P_S), where the characteristic [102], submerged [78, 58] and total surface area [86, 54] have been employed.
4. PTO force (i.e. the group $P_{F_{PTO}}$) has been used in [102] to represent the efficiency of mechanical to electrical power conversion in terms of its RMS value. Additionally, the reaction forces on the hinge of a pitching device were used in the objective function to be minimised in [78].
5. Displacement (i.e. the group P_{RAO}), where the RAO has been used to constrain the maximal oscillation. McCabe et al. include oscillation velocity, as a representation of the excursion, in the denominator of the objective function to be minimised in [53]. In [55] McCabe uses a different strategy calculating a time series of the oscillation to constrain the total stroke. In contrast, some studies with more simple objective functions have aimed at maximising the oscillation as a representation of the power, such as in [38] and [40].

A preliminary study comparing the use of different objective functions in WEC hull geometry optimisation was presented in [61], where it was found that surface area was a better representative for costs than volume when using a flexible geometry definition (such as in geometry (n) in Figure 3). However, when using simple shapes little difference was found in the optimisation results when applying volume versus surface area based cost proxies [58]. Mass and volume can be considered equivalent in this context, given that the displaced water mass can be represented through the submerged volume and the density of water. Where the RAO has been used to constrain the stroke of oscillation, this is comparable with studies aiming at minimisng PTO force, as mentioned in [112]. The efficiency and effectiveness of these latter methods to generate shapes with increased PTO reliability is not clear.

Overall, the use of AEP or mean annual absorbed power rather than CW, CWR, oscillation RAO or velocity is preferred. This is because: 1) the behaviour of the device is highly dependent on the resource and evaluating a device at a single wave height and period is not representative of its behaviour in a real sea. Optimisation procedures using these approaches tend to converge to devices with a natural period equivalent to the studied wave period (e.g. [70]). 2) the device performance will vary depending on the power absorption capabilities of the device. This cannot be taken into account when using RAO or velocity. Even if an optimal control is used as in [55], rather than a more realistic control as suggested in [6], this allows to consider an upper limit of the AEP. 3) certain measures of the device, such as the submerged volume, can be constrained to avoid the optimisation on converging towards very big or very small devices, depending on the objective function. In this way, the use of device dependent measures in the objective function, such as the characteristic length, can be avoided.

Additional effects that have been considered for their impact on costs are the loads on the device structure. The simplest way to study hydrodynamic loads is by analysing the pressure distribution on the structure from Boundary Element Method (BEM) based analysis results. In this way, hydrostatic and hydrodynamic pressures on the surface can be calculated for small incident waves and device oscillations [76]. To consider further structural requirements and extreme load cases, Finite Element Methods (FEM) have been used, for example in [37] or in [113, 114, 115], where different modelling methods for extreme, structural and design loads are investigated. An example comparison of two different float and mooring system combinations based on structural and extreme loads is given in [48]. Very general guidelines for structural assessment of WECs have been given in [116] and device specific studies are only available for the Pelamis [81] and SeaWave [82] machines, where the suitability of different materials was investigated. A more recent review of structural integrity analysis methods for WEC design was published by Coe et al. [117]. Some of the methods reviewed in this study have been implemented in the WDRT toolbox [118]. These types of structural loads have not been considered within hull geometry optimisation. A method offering the right trade-off between computational accuracy and time needs to be found for this purpose.

Other factors have been considered for their influence on the optimal device shape. A preliminary study on how to include material choice and manufacturability considerations in WEC geometry optimisation processes was presented in [59], which includes considerations from ship hull design for manufacturability [12] using developable surfaces. The effects of the chosen modes of motion for energy extraction on optimal geometries were also studied in [60]. These modes were shown to have a large impact on the preferred shapes, which tended to show increased surface areas perpendicular to the modes of motion for power extraction.

An overview of the metrics involved in geometry comparison and geometry optimisation studies is given in Table 3.

Table 3: Studies using each of the described metrics in their objective functions.

Metric	Description	Unit	Relevant comparison studies	Relevant optimisation studies
AEP	Annual Energy Production	[kWh], [kW]	[26], [72]	[51], [85], [96], [55], [59], [60], [63]
$\bar{P}$	Mean power	[kW]	[34], [65], [71], [47], [83]	[52], [69]
η	Efficiency based on radiated field	[%]	[33], [39]	-
CW	Capture Width	[m]	[46], [66], [50]	[91]
CWR	Capture Width Ratio	[%]	[87], [35], [70], [65], [64], [41], [43], [77], [26], [45], [89], [80], [83], [49], [72]	[84], [92, 93, 94, 95], [68], [79], [62]
P_m	Performance per unit mass	[kWh/kg] or [kW/kg]	[76], [41], [48]	[97], [57], [62]
P_V	Performance per unit volume	[MWh/m^3] or [MW/m^3]	[88], [42], [43], [44]	[73], [74], [55], [56], [75], [58], [59], [60], [63]
P_S	Performance per unit surface area	[MWh/m^2] [MW/m^2]	[88], [48]	[86], [54], [78], [58], [63]
$P_{F_{PTO}}$	Performance per unit PTO force	[kWh/N]	[102]	[78]
P_{RAO}	Performance per unit displacement characteristic	varies	-	[53]
RAO	Response Amplitude Operator		[36], [66],[50]	[51]
$\dot{X}$	Velocity	[m/s]	[38], [40]	-
F	Loads	[N]	[81], [37], [77], [82], [48]	-

3.4. Optimisation procedure

Different optimisation algorithms exist to find solutions to both single and multi-objective optimisation problems. Exact methods obtain optimal solutions and can guarantee their optimality (e.g. the pattern search, and simplex methods). These include gradient-based methods, which require the objective function to be differentiable, but also direct search methods, which are gradient-free. Approximate methods can find good solutions to complex problems, but do not have an approximation guarantee on the obtained solution. Heuristic algorithms fall into this category and are developed to solve a specific problem, whereas metaheuristic methods are generally-formulated algorithms to solve different kinds of optimisation problems (e.g. evolutionary algorithms, such as, evolution strategies and genetic algorithms).

Further differentiation between single-solution and population-based methods can be made. Single-solution methods applied to a single-objective or multi-objective problem will find one solution for each run of the algorithm. Population-based methods deal simultaneously with a set of solutions and can find several single-objective solutions or several members of the Pareto optimal set [3] in a single run of the algorithm. Population-based metaheuristics are also less sensitive to the shape of the Pareto front.

As a result of the above characteristics, the use of metaheuristic algorithms, and particularly of Genetic Algorithms (GAs), has become very popular for their application in WEC geometry optimisation problems. That is, they are better suited to solve complex problems, are able to find solutions to non-convex problems and being population-based, can analyse more of the solution space in less algorithm runs. What a convex versus a non-convex optimisation problem looks like is represented through two Pareto Fronts in Figure 4[4]. To allow for a general understanding of GAs' functioning, these are described in some more detail below.

[3] Results from a multi-objective optimisation iteration are called Pareto optimal set. This set of results should converge towards the true Pareto Front within the optimisation process.

[4] This is represented for multi-objective cases, but if $f_2(x)$ is replaced by x, the figure would show convexity for an optimisation problem with one objective function. Convexity is also a characteristic of the optimisation constraints, but this is not discussed here.

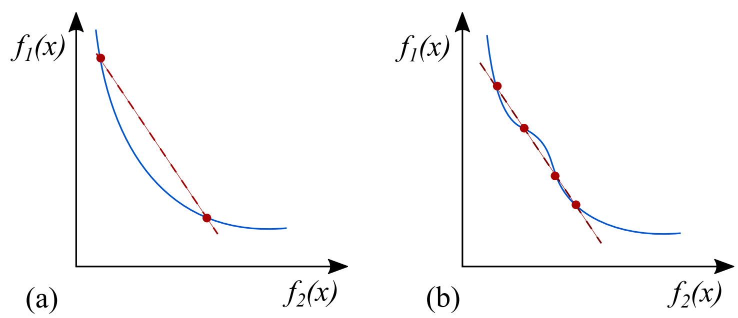

Figure 4: Representation of convexity in the Pareto Front in multi-objective optimisation problems. (a) is a convex, and (b) a non-convex Pareto Front.

Genetic Algorithms were first proposed by Holland [119] and a good overview of their different variations can be found in [30]. Genetic algorithms make use of evolution theory, featuring the survival of the fittest individuals within a population. The initial population, in the currently analysed case, is a set of WEC shapes represented by random combinations of the decision variables (e.g. diameter and draft). The geometries are assessed based on an objective function, for example, the mean power output over a year for a given location and new geometries are generated through selection, recombination and mutation processes. The different steps of a generic GA are represented schematically in Figure 5.

Many different algorithms exist for the fitness assignment, selection, recombination and mutation operations, and parameters such as the mutation rate or the number of individuals per generation, need to be tuned to ensure the correct functioning of the algorithm. The goal is to allow for a wide search of the optimisation space, without preventing the algorithm from converging. Therefore, the algorithm should be able to identify better solutions and allow for a refined search around those points. This is often referred to in optimisation as finding the right balance between exploration and exploitation.

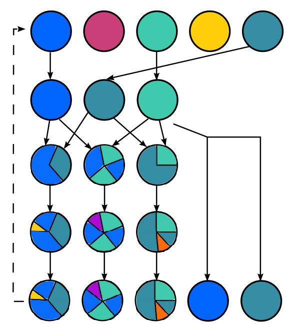

Figure 5: Representation of a genetic algorithm iteration.

Within a multi-objective optimisation process, different strategies exist to recognize better performing individuals. Most commonly the concept of Pareto dominance is used. One solution is said to dominate another one when it performs better in all, or is equally good but better in at least one, of its objective functions' values:

$$\forall i \in 1, ..., n : f_i(\mathbf{x}) \leq f_i(\mathbf{y}) \wedge \exists i \in 1, ..., n : f_i(\mathbf{x}) < f_i(\mathbf{y}), \tag{14}$$

where $\mathbf{x}$ and $\mathbf{y}$ are vectors containing the decision variables that represent two different solutions.

Some of the geometry optimisation studies analyse the suitability of the employed optimisation algorithms. This is the case, for example, in Gomes et al. [96] and Ribeiro et al. [97] where the suitability of two algorithms for the hydrodynamic optimisation of a WEC was investigated. For that particular case, it was found that the search method 'Constrained optimisation BY Linear Approximation' (COBYLA) based on the simplex method provided good solutions with less computational effort than the 'Differential Evolution' (DE) algorithm. However, it should be noted that the final solution obtained with algorithms such as COBYLA and other direct search methods are highly sensitive to the initial solution guess. In most cases, where exact methods were applied to WEC geometry optimisation, these can be categorised as direct search methods which do not require the objective function to be differentiable, such as Simplex based methods [52, 96] or the simple pattern search algorithm [86]. A single variable optimisation approach was used in [75], where the optimal scaling factor for a set geometry in different sea conditions was sought. In general, in cases with a reduced number of decision variables and where informed initial guesses for good solutions can be made, direct search methods might be preferred. For more complex problems, metaheuristic algorithms are recommended. The most suitable optimisation algorithm for different WEC geometry single-objective optimisation formulations was studied in [63]. Preferred algorithm implementations were found depending on the used objective function and the number of modes-of-motion considered for power extraction with improvements in final objective function values of up to 11% when using the most suitable algorithm. Regarding the formulation of multi-objective optimisation problems, Koh et al. [43] identified a non-convex region in their approximated Pareto front for the relation between mean absorbed power and volume. When using a weighting approach to create a single-objective function combining various objectives, solutions to non-convex problems might not be found. Multi-objective population-based algorithms are more suitable for this type of problem. An overview of the employed algorithms in the different studies is given in Table 4.

Table 4: Studies using the different types of the optimisation algorithms.

Optimisation Problem	**Method**	**References**
Single objective	Exact	[84], [52], [86], [96], [97] , [75]
	Metaheuristic	[73] , [85], [96] ,[55], [97] , [57], [80], [99], [59], [60], [69], [62], [63]
Multi-objective	Exact	-
	Metaheuristic	[51], [53], [54], [78], [74] , [56], [58]

4. Geometry of wave energy converters

In this section, geometry comparison and optimisation studies are reviewed so that a reader interested in previous studies for particular types of devices can find more detailed information on findings and approaches for specific technologies. Here comparison studies are used to give an insight on preferred shapes and modelling methods, whereas optimisation studies provide information on optimisation problem formulations and methods to speed up the objective function evaluation.

4.1. Geometry comparison studies

Various studies on the effects of geometry on WEC performance have been carried out, where a discrete number of WEC geometries were compared to each other without going through an actual optimisation process. An overview of these studies is given in Table 5.

4.1.1. Heaving vertical cylinders

Heaving vertical cylinders have been studied extensively. From these studies it can be concluded that: 1) an optimal combination of radius and draft exists for a given wave amplitude and frequency [34]. In that particular case, it was found that the optimal surface radius increased with increasing draft, and with the normalised displacement amplitude. 2) for low wave frequencies in general bigger devices perform better because they tend to have lower natural frequencies and vice versa [41, 49][5]. 3) the power-to-volume Pareto front has non-convex regions and actual multi-objective optimisation (not weighted single-objective) formulations need to be used to find a solution that approaches the true Pareto Front [43]; and 4) the used control strategy can reduce the WEC hull size and increase the resonance bandwidth [42, 44].

4.1.2. Heaving modified vertical cylinders

Variations in the cylinder bottoms have been studied to analyse reductions in viscous effects and improvements in power absorption. Overall, these comparative studies show that: 1) when using CW, CWR and RAO, the preferred shapes are those with their natural period closest to the studied periods of the wave resource and tend to favour shapes of larger volume [38, 70]; 2) the resonance bandwidth is smallest for the flat-bottomed cylinder and larger for streamlined or parabolic cone shape bottoms (i.e. geometry type (d) in Figure 3) [47, 50]; 3) when considering viscosity effects, radiation damping can be increased up to 60% [36], and 4) shapes with deadrise angles larger than zero show better performance, where a 90° apex angle was recommended for bottom slamming considerations [35] (see Figure 6 for angle definitions).

[5]Note, however, that for instance a thin cylinder with a large draft has a low natural frequency in heave

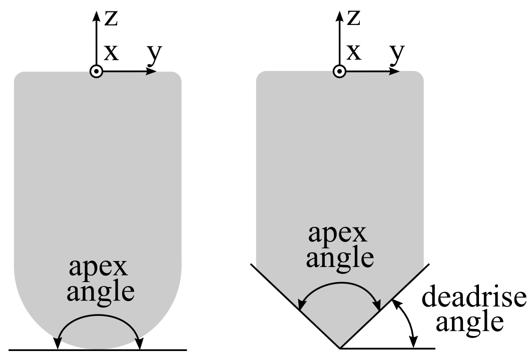

Figure 6: Representation of apex and deadrise angles.

4.1.3. Other devices

The geometry of other device types has been studied to a lesser extent and it is therefore difficult to draw conclusions from studies' comparison.

An interesting study was performed by Yu el al. [76], where the device's mass was determined based on the pressure distribution on its surface. In this way the device design was ensured to withstand the wave loading. This highlights the idea that although general device design can be determined through optimisation, certain characteristics can be defined through design requirements, as was done in that study. Three different designs of flap-type oscillating wave surge energy converters were compared in [76]: a single flap, two flaps side by side, and a fore and aft flap, represented in Figure 7 D-I to III, respectively. Pressure distributions calculated by the BEM software WAMIT were used to determine the minimum thickness of the steel tubes forming the supporting frame and the fiberglass tubes forming the flaps by applying simple beam theory. A WEC-Sim model was built to analyse the power performance of these devices, which were then compared based on their AEP to characteristic mass ratio, where mass represented a proxy for costs. The best results were obtained with the fore and aft flaps design with slack mooring. Taut moorings achieved better performance than slack moorings for the other two designs. An oscillating wave surge energy converter composed of various controllable flaps was introduced by Tom et al. [77] (see Figure 7 D-IV), with the aim of maximising power and reducing design loads through geometry control. A non-linear model was used for the evaluation of this type of device and it demonstrated an improved performance potential with increased capacity factor and reduced hydrodynamic loads in regular waves.

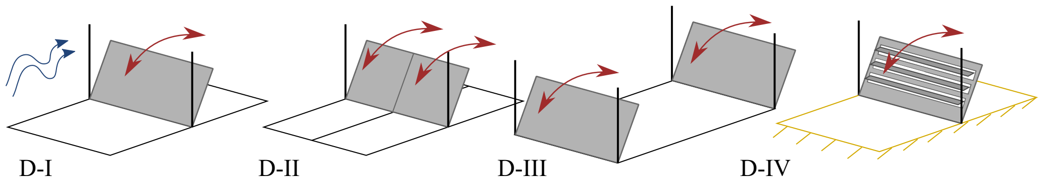

Figure 7: Schematic representation of various flap devices. Adapted from [76] and [77].

4.2. Geometry optimisation studies

An overview of different hull geometry optimisation studies is given here and is summarised in Table 6.

4.2.1. Point absorbers with 'simple' shapes

Point absorbers with simple shapes have been used to study the interaction of joint optimisation of geometry and control strategy for the PTO-system.

The effect of the employed control strategy was studied within a geometry optimisation process in [52]. In that study, Gilloteaux and Ringwood investigated the optimal dimensions of a vertical cylinder with and without latching control, based on mean absorbed power for a specific sea state using the Simplex algorithm. Optimal devices for the case without control had approximately double the radius and draft of the devices for the case with latching control.

Barbarit et al. [51] optimised the shape of the SEAREV WEC, composed of a pendulum enclosed in a floating hull oscillating in heave, surge and pitch. Three different shape families were studied where the characteristic lengths - length, beam, draft and vertical position of the center of gravity - were chosen as the decision variables. Using a frequency-domain method, the shapes were optimised in a multi-objective optimisation process with the help of genetic algorithms to maximise the AEP and minimise the submerged volume as a representative of the costs. In an inner loop optimisation process, the optimal pendulum for each shape was found using a gradient method.

The optimisation results show potential to reduce hull size, when optimising the PTO control strategy and geometry simultaneously. The nested optimisation approach suggested in [51, 52] proves suitable for this purpose, where an optimal PTO design and control strategy will exist for each shape.

Table 5: Overview of WEC geometry comparison studies

WEC type	Shape	Metric	Analysis	Institution	Reference
(A) point absorber - single body - floating	NA	η	Frequency-domain	Unknown	[33]
	(a)	$\bar{P}$	Numerical	Wave Energy Centre (WavEC)	[34]
	(b), (d)	CWR	Frequency and time-domain and experimental	Ghent University	[35]
	(a)	$\bar{P}$, P_V	Pseudo-spectral	Maynooth University	[42, 44]
	(a), (b), (c), (d)	RAO	Numerical (FSRVM)	University of California at Berkeley	[36]
	(b), (i), (j)	F	Time-domain and FEM	Polytechnic Institute of Coimbra	[37]
	(a), (d), (f), (g), (i)	$\dot{X}$	Frequency-domain	National University of Ireland	[38]
	(e), (o)	CW, η	Frequency-domain and CFD and experimental	University of California	[39, 46]
	(a)	$\dot{X}$	Frequency-domain and experimental	Uppsala University	[40]
	(a)	CWR, P_m	Frequency-domain	University of Cantabria	[41]
	(o)	AEP, CWR	Analytical (Scaling)	University of Edinburgh	[26]
	(a)	CWR, P_V	Frequency-domain	Jeju National University	[43]
	(a), (b), (d)	CWR	Time-domain	University of Twente	[45]
	(a), (b), (d)	$\bar{P}$	Numerical	Harbin Engineering University	[47]
	(a), (b), (d)	P_m, P_S, F	Time-domain and CFD	National Renewable Energy Laboratories	[48]
	(a)	CWR	Frequency-domain	Federal University of Rio de Janeiro	[49]
	(a), (b), (d)	CW, RAO	CFD	University of Hull	[50]
(B) point absorber - single body - submerged	(j)	CWR, F	Frequency-domain	University of Bristol	[65]
	(a), (o)	CWR	Time-domain	University of Cantabria	[64]
	(o)	CWR, RAO	Frequency-domain	Plymouth University	[66]
(C) point absorber - two body	(a), (b), (h)	CWR	Time-domain	National Technical University of Athens	[70]
	(f), (o)	$\bar{P}$	Frequency-domain and experimental	University of Victoria	[71]
	(a), (o)	CWR, AEP	Frequency and time-domain and experimental	Aalborg University	[72]
(D) terminator - hinged flap	(m)	P_m	Time-domain	National Renewable Energy Laboratory	[76]
	(m)	CWR, F	Time-domain	National Renewable Energy Laboratory	[77]
(E) attenuator	(j)	F	Analytical	Ocean Power Delivery Ltd.	[81]
	(j)	F	Experimental	Plymouth University	[82]
	(l)	CWR, $\bar{P}$	Frequency-domain	University of Bristol	[83]
(F) oscillating water column	(o)	CWR	Experimental	The Queen's University of Belfast	[87]
	(o)	P_V, P_S	Frequency-domain	Technical University of Lisbon	[88]
	(o)	CWR	Numerical and experimental	Istanbul Technical University	[89]
	(o)	NA	Numerical and experimental	University of Bologna	[90]

4.2.2. Other single-body floating point-absorbers

For other single-body floating point-absorber type devices, the focus of geometry optimisation has been on employing more adaptable geometry defintions to improve the variation potential of the obtained solutions. Overall, adaptable geometry definitions proved to be particularly important in geometry optimisation studies, to generate more diverse and better performing shapes [55, 78, 57, 59, 60, 63]. In combination with more adaptable shape definitions, surface area based cost proxies in the objective function have shown to generate more realistic and suitable shapes than volume based cost proxies [59, 61]. The submerged surface area was found to generate less-complex shapes of larger cross-section, which would enable better load distribution and easier manufacturing and reinforcement.

4.2.3. Two-dody floating point-absorbers

Multiple studies have been performed by Blanco et al. on the optimisation of two-body floating point absorbers, mostly following the examples represented in Figure 8, but also in comparison with more simple shapes such as a vertical cylinder. Some interesting considerations mentioned in these studies, include taking into account different WEC resonance strategies in [56], where 1) the WEC resonance frequency matches the sea state with the highest occurrence - multiple resonance frequencies can be found for the two-body case, 2) only the highest resonance frequency is taken into account, and 3) this is not taken into account as a constraint. Additionally, multiple constraints on the WEC operation were applied in [58], for example, regarding minimum electrical generated power or anti-slamming considerations. However, all of them were defined through relaxation coefficients, which gave the different constraints different weights, but which were not specifically defined in the publication. This more holistic perspective applied to WEC optimisation considering different operating conditions and operational constraints can be very valuable to ensure that device designs are optimised for the particular conditions the WEC is expected to be operating in while avoiding hull damaging responses in those conditions.

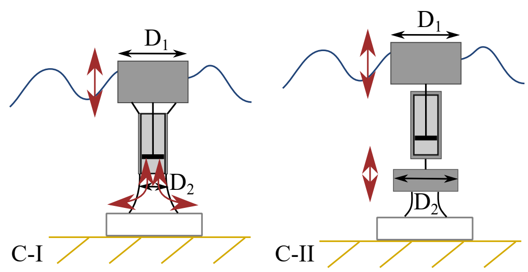

Figure 8: Two-body wave energy converters. C-I represents the IPS buoy and is adapted from [73] and C-II was adapted from [56].

4.2.4. Other devices

A flap type oscillating wave surge converter (OWSC) (as shown in Figure 2 D) was optimised in [80], where flap width, water depth, and hinge height were varied to maximise the CWR at a generic North Atlantic location, and the results were compared with past OWSC prototypes. The hydrodynamic characteristics were obtained through a semi-analytical model for oscillating flap type devices developed in [120]. Results showed that greater hinge heights and smaller flap widths than used in previous devices generated better results at lower water depths. It was also found that flap width had the least influence on performance.

An extensive review on turbine design optimisation for Oscillating Water Column type WECs is given in [98], where both Wells and impulse turbines are considered. An example study can be found in [99], where Mishra et al. used Particle Swarm Optimisation (PSO) to optimise the rotor resistance of an OWC Wells turbine controlled with Maximum Power Point Tracking (MPPT). The purpose of this was to avoid stall and reduce power losses. In addition, studies of the spar buoy geometry of OWC converters have been performed, such as in [96]. Simultaneous optimisation of the turbine characteristics and the device geometry have been extensively discussed by Weber et al. [93, 94, 95].

5. Summary

5.1. Is there a preferred shape?

Of the shapes studied for single-body heaving devices, spherical hull shapes seem to be more suitable for structural integrity with regards to stress concentration, according to [37]. However, spherical bottoms result

Table 6: Overview of WEC geometry optimisation studies

WEC type	Shape	Metric	Optimisation Algorithm	Analysis	Institution	Reference
(A) point absorber - single body - floating	(j), (l), (o)	AEP, RAO	Multi-objective, Metaheuristic	Frequency-domain	Ecole Centrale de Nantes	[51]
	(a)	$\bar{P}$	Single-objective, Exact	Time-domain	National University of Ireland Maynooth	[52]
	(n)	P_{RAO}	Multi-objective, Metaheuristic	Frequency-domain	Lancaster University	[53]
	(k)	P_S	Multi-objective, Metaheuristic	Frequency-domain	Norwegian University of Science and Technology	[54]
	(n)	AEP, P_V	Multi-objective, Metaheuristic	Frequency-domain	Lancaster University	[55]
	(a)	P_V, P_S	Multi-objective, Metaheuristic	Frequency-domain	CIEMAT	[56, 58]
	(e)	P_m	Single-objective, Metaheuristic	Pseudo-spectral	Michigan Technological University	[57]
	(n)	AEP, P_V, P_S	Single-objective, Metaheuristic	Frequency-domain	University of Edinburgh	[59, 60, 61, 63]
	(o)	P_m, CWR	Single-objective, Metaheuristic	Frequency-domain	Politecnico di Torino	[62]
(B) point absorber - single body - submerged	(j)	CW	Single-objective, Not specified	Frequency-domain	University College Cork	[67]
	(j)	CWR ($\bar{P}$)	Single-objective, Not specified	Frequency-domain	University of Bristol	[68]
	(a), (n)	$\bar{P}$	Single-objective, Metaheuristic	Frequency-domain	Stanford University	[69]
(C) point absorber - two body	(o)	P_V	Single-objective, Exact & Metaheuristic	Frequency-domain	Technical University of Lisbon	[73]
	(a), (b), (o)	P_V	Multi-objective, Metaheuristic	Frequency-domain	CIEMAT	[74, 56]
	(o)	P_V	Single-objective, Exact	Frequency-domain	Sandia National Laboratories	[75]
(D) terminator - hinged flap	(i), (m)	$P_S, P_{F_{PTO}}, F$	Multi-objective, Metaheuristic	Frequency-domain	Norwegian University of Science and Technology	[78]
	(m)	CWR	Single-objective, Not specified	Frequency-domain	University of Bristol	[79]
	(m)	CWR	Single-objective, Metaheuristic	Frequency-domain	Loughborough University	[80]
(E) attenuator	(l)	CWR	Single-objective, Not specified	Frequency-domain	Massachusetts Institute of Technology	[84]
	(o)	AEP	Single-objective, Exact	Time-domain	Oregon State University	[85]
	(l)	P_S	Single-objective, Metaheuristic	Frequency-domain	National University of Ireland Maynooth	[86]
(F) oscillating water column	(l)	CW	Single-objective, Not specified	Frequency-domain	University of Bristol	[91]
	(o)	CWR	Single-objective, Exact	Time-domain	University College Cork	[92, 93, 94, 95]
	(o)	AEP	Single-objective, Exact	Frequency-domain	Technical University of Lisbon	[96]
	(o)	P_m	Single-objective, Exact & Metaheuristic	Frequency-domain	Technical University of Lisbon	[97]
	NA	NA	NA	Review	Indian Institute of Technology Madras	[98]
	NA	NA	Single-objective, Metaheuristic	NA	Motilal Nehru National Institute of Technology	[99]

in larger slamming coefficients due to the small deadrise angle [35]. For this reason, cone-shaped bottoms are preferred for slamming and drag considerations, where streamlined cone-shapes show the best performance in terms of maximising power and minimising drag losses [35, 36, 45, 38]. These were also found to perform well over larger bandwidths when compared to flat-bottomed cylinders [47]. This might, however, not apply when considering irregular waves of wide bandwidth [50]. Otherwise, many of the findings were influenced by the considered period ranges and shape volumes, and might not be generally applicable.

The influence of geometry on forces is not clear from the available literature. The choice of mooring lines and PTO-system will have an impact on the system dynamics and will affect the hydrodynamic loads experienced by the structure.

5.2. How do I optimise my device design?

To optimise a device design, the key elements of the geometry optimisation formulation need to be defined (see section 3).

First, for a given geometry definition, the decision variables to be optimised, and their bounds, as well as any other design constraints need to be identified. In this context, the use of Bézier curves and B-spline based geometry definitions has proven to be better suited for a more adaptable geometry definition, which is capable of generating enhanced solutions [55, 57]. However, to ensure the selection of shapes that truly reduce the LCOE, more advanced objective functions and constraints are required that reflect the desired and undesired characteristics of these shapes, such as penalising increases in viscous drag or manufacturing complexity. An example of the latter was discussed in [59], and additional constraints are discussed in [63].

Secondly, the metrics to be used in the objective function need to be defined and the required modelling approach implemented. Results of studies using CW, CWR, velocity or displacement, as representatives for power generation performance, are difficult to compare consistently with other studies. The use of AEP rather than oscillation velocity or displacement is recommended, to account for further effects of the system dynamics, such as the PTO-system. The use of irregular waves and the representation of various sea states is also preferred, since optimal shapes will vary with sea conditions. It was shown from the reviewed studies that, when considering single sea states or small period ranges, shapes with a natural period matching the studied conditions will be favoured, which might not be optimal for real sea conditions. To avoid the use of device dependent measures (e.g. characteristic length) in the objective function, the size can be limited through more device agnostic measures such as submerged surface area or submerged volume. Preliminary results show a preference for submerged surface area as a proxy for costs in combination with complex shape definitions [61], although little difference in optimisation results was found for simple shapes when using submerged surface area or submerged volume [58].

Finally, the optimisation of the geometry, in combination with the PTO and control systems, shows potential for improved power absorption capability [6, 42, 44] and reduced floater size [52]. For this reason, it is recommended to perform a 2-layer optimisation, in which the optimal PTO characteristics are calculated in an inner optimisation loop for each geometry - optimised in an outer optimisation loop, as suggested in [52]. This has also been performed for simulteanous geometry and PTO optimisation without a focus on the control strategy in [51, 62].

5.3. What tools are available?

Wave energy converter optimisation tools are not readily available. However, a range of tools for optimisation and for hydrodynamic modelling of WECs exist.

In terms of optimisation tools, a wide range of readily implemented optimisation algorithms exist in commonly used languages such as Matlab and Python. This can be used in combination with parallel computing tools, so that the computational time of the optimisation can be reduced. Specific software packages for optimisation purposes also exist such as modeFRONTIER [121]. All of these tools are equally convenient for this purpose, so that the choice will depend on software accessibility and availability, where Python has the advantage of being open-source.

In terms of hydrodynamic modelling tools, a range of codes exist for the computation of the hydrodynamic coefficients of the different shapes. Nemoh [122] is an open-source BEM based tool that uses panel discretisation for the computation of the hydrodynamic characteristics. Its capabilities have been verified and validated in multiple studies. The main disadvantage might be the limited amount of documentation for its use. The commercial software WAMIT [123] is a more versatile tool for the same purpose, that allows the use of panel discretisation, but contains also the 'Higher-Order Method', which uses B-splines to calculate a continuous solution of the velocity potential over the submerged surface. This option offers a great advantage in terms of computational time for the evaluation of complex shapes, where otherwise a very refined discretisation is necessary. The tool is well documented in its manual. This tool is recommended for the evaluation of more complex shapes to reduce computational time. Another commercial package Ansys Aqwa [124] offers similar functionality to Nemoh, with the added value that it can then be easily connected with Ansys' other functionalities such as Computational Fluid Dynamics (CFD) analysis.

5.4. How fast can I get my result?

The optimisation time will highly depend on 1) the capabilities of the machine or server used for the computation, 2) the employed objective function and modelling approach, and 3) the chosen optimisation algorithm and its implementation.

For example purposes, approximated run times for different performance calculations are given in Table 7 based on the results obtained on an i7 computer with 32GB of RAM when using WAMIT with the Higher-Order method for a single cylindrical floating body. The corresponding optimisation run times when using a genetic algorithm with 25 individuals for 100 generations without any parallelisation of the calculation are provided. For this calculation, it is assumed that 2 elite individuals are being reinserted and 23 new individuals evaluated in every iteration. The values for the time-domain model are approximated based on [125, 126, 127], where the time-domain modelling open-source software WEC-Sim [128] was used to model single sea states. The time for analysing 100 sea states was assumed to scale linearly. Example computation times for, both, regular sea representations, where only one frequency per sea state was evaluated, and for irregular sea representations, where 150 frequencies were considered, are provided. It should be noted that parallelisation can be used so that the run time can be significantly reduced. For example, 5 parallel WAMIT runs can be performed simultaneously on an i7 computer. If the power calculation can be parallelised to the same extent, then a fifth of the approximated optimisation time can be assumed. For the frequency-domain and the pseudo time-domain models, the largest contribution to the computation time stems from WAMIT, which increases for irregular sea state representations, due to the increased number of frequencies being evaluated.

Table 7: Approximated expected run times depending on modelling approach. Values for the evaluation of single shapes are recorded under 'Single', whereas values for a theoretical optimisation are listed under 'Opt.'.

Resource representation	**Frequency domain**		**Pseudo time domain**		**Time domain**	
	Single	Opt.	Single	Opt.	Single	Opt.
1 Sea state, regular	3 s	1.9 h	3 s	1.9 h	15 min	24 d
1 Sea state, irregular	49 s	31.3 h	49 s	31.3 h	3 h	288 d
100 Sea states, regular	10 s	6.4 h	11 s	7.0 h	150 min	240 d
100 Sea states, irregular	52 s	33.3 h	68 s	43.5 h	300 h	28775 d

5.4.1. Speed-up methods

The large computational times of this type of optimisation process were identified as a challenge in most of the reviewed literature and different approaches were used to get around this problem. For example, a reduced number of sea states were analysed in [70, 74, 56, 96], but the effect that this simplification can have on the results should be studied further. An example of a method for reduced sea state selection was proposed in [129].

Zhang et al. [47] introduced a semi-analytical method to more efficiently obtain hydrodynamic coefficients within a geometry optimisation process. In this respect, the use of the Higher-Order-Method offered in the WAMIT software, instead of the Low-Order panel method, for the calculation of hydrodynamic coefficients, can result in a substantial acceleration of the optimisation process.

Speed-up is also achieved through problem simplification, such as using frequency-domain models instead of time-domain models, or regular waves instead of irregular waves to represent the available resource. In addition, less complex objective functions can be used, such as device velocities instead of the AEP. The suitability of the modelling approach should be validated experimentally. The other simplifications mentioned here are not recommended and the effect that these have on the results need to be investigated further before conclusions can be drawn from these studies.

Another mechanism for reducing computational time was the use of surrogate models, so that the calculation of hydrodynamic coefficients by BEMs was not required. This is the case in [43], where a Response Surface Method (RSM) was used to accelerate the search. This method enables the construction of approximations to the system behaviour based on the pre-analysis of various design variable combinations [130]. Similarly, neural networks were used in [85] to predict power output based on mass properties. However, the use of these methods is linked to inaccuracies of the system representation, which will increase with system complexity. Finding a trade-off between model accuracy and computational time is one of the key challenges when setting up an optimisation problem.

The choice of optimisation algorithm and its tuning can also have a significant influence on the computational time. If a fast converging algorithm (i.e. achieving consistent and close to optimal results) is applied, a lot of time can be saved through a reduced number of function evaluations, without reducing the modelling accuracy.

It is recommended to ensure the correct selection of the optimisation algorithm and its tuning, before any model simplifications are used to achieve speed-up of the optimisation. If model simplifications are used, their effect on the optimisation results should be investigated and understood, as far as possible, to allow for the correct interpretation of the optimisation results.

5.5. What are the improvements achieved through optimal device design?

Device designs generated through an optimisation process have been compared to different benchmark shapes. In [55] improvements of up to 4 times the objective function value obtained with a barge shape of the same submerged volume were achieved, when accounting for costs in the objective function using volume as a proxy. In [69] improvements in mean power of up to 6 times the mean power produced by a submerged flat cylinder-shaped device of the same cross-sectional area were achieved. In [61] it can be seen that different trade-offs of power and costs are achieved when using different cost proxies. It is discussed in that article that it is, therefore, important to use representative cost proxies to ensure that the generated shapes truly represent shapes that will result in LCOE reductions. However, it is also difficult to prove what is the most suitable formulation for this purpose.

In the study by Kurniawan et al. [72], a parametric investigation for a two-body device was carried out and a design was selected based on a frequency-domain model. The selected device design was then tested experimentally and modelled in the time domain. It was shown that a pitch/roll instability that had not been captured in the frequency-domain model, resulted in a reduced power production in reality. Since the same tests and modelling was not performed for the reference device it is difficult to state if there was any improvement in the new device design. However, the results of this study point to the need for validating the models used for geometry optimisation to ensure that the selected shapes do perform better overall.

6. Conclusions and recommendations for future research

Geometry optimisation of wave energy converters has been extensively studied, due to the valuable insights it provides for device design, and due to its potential to generate novel and improved designs avoiding expensive iterations at later stages.

6.1. Conclusions

Based on the studies reviewed here, the following conclusions could be drawn regarding best practices:

- **Choice of geometry definition**
  Using predefined shapes of variable dimensions can be very restrictive on the optimisation results. For flexibility, the use of B-spline surfaces, such as in [55], and polynomial functions, such as in [57], is recommended [63].

- **Choice of objective function**
  The use of AEP or mean annual power to represent power absorption performance is recommended. For more accurate power performance results, PTO-constraints involving stroke, power rating, and forces should be included. The PTO and control systems will highly influence the device dynamics, and therefore the optimal shape as well [42, 44]. The simultaneous optimisation of geometry and control strategy should be considered in the future, as shown in [52].

  Volume has proven to be a bad proxy for costs in combination with complex geometry definitions. Surface area, or surface area in combination with wall thickness, as a representation of mass, can lead to more realistic results, as suggested in [59, 131]. However, for simple shapes, little difference was observed in optimisation results when using submerged volume or submerged surface area [58].

Slamming effects can be incorporated as described in [35]. The inclusion of other structural integrity considerations needs to be investigated further.

Viscosity and drag effects will vary with geometry, and should be accounted for when possible. However, to obtain viscous drag coefficients of complex shapes, CFD simulations are required which might result in a prohibitive increase in the computational effort for an optimisation process.

- **Choice of optimisation algorithm**
  Metaheuristic algorithms are, in general, more suitable for evaluating complex problems, such as WEC geometry optimisation problems with complicated shapes or objective functions. In the case of multi-objective studies, the representation of multiple objectives in a single-objective weighted sum is discouraged, since this could cause the algorithm to evaluate non-convex solution space regions incorrectly. Additionally, the chosen weighting of the different objectives is highly subjective and will affect the results. For single-objective WEC geometry optimisation problems, preferred algorihtm implementations for different cases were found in [63]. In all cases, a preliminary study to tune algorithm parameters is recommended to improve convergence to the global optimum.

6.2. Future research

Despite the wide-ranging learnings obtained from the reviewed literature, some research gaps were identified that should be addressed in the future to gain further insights into optimal wave energy converter design. Some of these are listed below:

- **Study the suitability of the optimisation formulation to define guidelines**
  This includes assessing the suitability of the identified key elements, such as the geometry definition, the objective function, the optimisation algorithms and the problem formulation, as well as the interaction of these elements. This will help to establish the best practices for wave energy converter design optimisation. An example for these type of

studies was provided in [63] for the choice of the geometry definition and the optimisation algorithm.

- **Combine geometry with control and power take-off system optimisation**
  Detailed control and PTO optimisation approaches have been studied extensively for WECs and have been used in combination with geometry optimisation based on simple shape definitions. Geometry optimisation models using more adaptable and complex geometry definitions should be combined with the extensively developed control optimisation approaches. This will allow to generate solutions with improved device dynamics and to gain a better understanding of the importance of these components and their contributions to power absorption.

- **Further study the effect of the used hydrodynamic model**
  This includes comparing optimal shapes when using different hydrodynamic models, and understanding for example, if frequency-domain models can be suitable for the generation of initial optimised designs or if more computationally demanding time-domain models are required to ensure the validity of the generated shapes.

- **Further study the effect of the wave climate representation and geographical location**
  This includes assessing the suitability of the methods for wave climate representation and reduction when used for wave energy converter optimisation, as well as the detailed study of the dependence of the results on location.

- **Further develop the inclusion of manufacturability considerations**
  Although preliminary studies exist [59], manufacturability of the optimised solutions has not been considered and should be investigated in more detail to ensure that the obtained geometries truly reduce the LCOE.

- **Further develop the inclusion of reliability considerations**
  Although preliminary studies exist [112], a suitable method for consideration of reliability in geometry optimisation of WECs should be studied further to allow for a more holistic preliminary design optimisation process. Simplified methods as presented in [112] should be

compared to more detailed PTO reliability studies and analysis methods to ensure their validity for this purpose.

7. Aknowledgements

The authors would like to thank the Energy Technology Partnership and UKCMER (EPSRC grants EP/I027912/1 and EP/P008682/1) for funding the Ph.D. project within which this work was performed.

References

[1] D. Bull, M. E. Ochs, D. L. Laird, B. Boren, R. A. Jepsen, Technological Cost-Reduction Pathways for Oscillating Water Column Wave Energy Converters in the Marine Hydrokinetic Environment (September) (2013) pp. 1–50. doi:10.2172/1092993.

[2] Strategic Initiative for Ocean Energy (SI OCEAN), Ocean Energy : Cost of Energy and Cost Reduction Opportunities, Tech. rep., SI OCEAN (2013).

[3] B. Teillant, R. Costello, J. Weber, J. Ringwood, Productivity and economic assessment of wave energy projects through operational simulations, Renewable Energy 48 (2012) 220–230. doi:10.1016/j.renene.2012.05.001.

[4] A. De Andres, E. Medina-Lopez, D. Crooks, O. Roberts, H. Jeffrey, On the reversed LCOE calculation: Design constraints for wave energy commercialization, International Journal of Marine Energy 18 (2017) 88–108. doi:10.1016/j.ijome.2017.03.008.

[5] M. French, R. Bracewell, Systematic design of economic wave energy converters, Proc. of the International Offshore and Polar Engineering Conference 1 (1996) 106–110.

[6] J. V. Ringwood, G. Bacelli, F. Fusco, Control, forecasting and optimisation for wave energy conversion, in: Proc. of the 19th World Congress of The International Federation of Automatic Control (IFAC), Vol. 19, IFAC, Cape Town, South Africa, 2014, pp. 7678–7689. doi:10.3182/20140824-6-ZA-1003.00517.

[7] L. Birk, S. Harries, Optimistic - Optimization in Marine Design, Mensch & Buch Verlag, 2003.

[8] G. Clauss, L. Birk, Hydrodynamic shape optimization of large offshore structures, Applied Ocean Research 18 (4) (1996) 157–171. `doi:10.1016/S0141-1187(96)00028-4`.

[9] L. Birk, Application of Constraint Multi-Objective Optimization to the Design of Offshore Structure Hulls, in: Proc. of International Conference on Offshore Mechanics and Arctic Engineering (OMAE), ASME, San Diego, CA, 2007, pp. 765–776. `doi:10.1115/OMAE2007-29625`.

[10] D. Eyres, A. Molland, H. Schneekluth, V. Bertram, R. Shenoi, A. Dodkins, D. Watson, Ship design, construction and operation, in: A. F. Molland (Ed.), The Maritime Engineering Reference Book - A Guide to Ship Design, Construction and Operation, Vol. 6, Elsevier Ltd, 2007, Ch. 9, pp. 638–727.

[11] J. S. Letcher, Geometry of Surfaces, in: J. R. Paulling (Ed.), The Geometry of Ships, Vol. I, The Society of Naval Architects and Marine Engineers, Jersey City, 2009, Ch. 4, pp. 30–46.

[12] U. Kilgore, Developable Hull Surfaces, Vol. 3, Fishing News (Books) Limited, London, 1967.

[13] G. Farin, N. Sapidis, Fairing Curves - Curvature and the Fairness of Curves and Surfaces, IEEE Computer Graphics and Applications (1989) 52–57`doi:10.1109/38.19051`.

[14] G. Chiandussi, G. Bugeda, Shape variable definition with C 0 , C 1 and C 2 continuity functions, Computer methods in applied mechanics and engineering 188 (2000) 727–742. `doi:10.1016/S0045-7825(99)00358-8`.

[15] J.-H. Nam, S. Sohn, D. J. Singer, Estimation of geometry-based manufacturing cost of complex offshore structures in early design stage, International Journal of Naval Architecture and Ocean Engineering 4 (3) (2012) 291–301. `doi:10.2478/IJNAOE-2013-0097`.

[16] G. Tampier B., M. Salas I., Hydrodynamic ship design for service conditions, Ocean Engineering 75 (2014) 23–29. doi:10.1016/j.oceaneng.2013.10.006.

[17] M. Ćurković, I. Marinić-Kragić, D. Vučina, A novel projection of open geometry into rectangular domain for 3D shape parameterization, Integrated Computer-Aided Engineering 25 (1) (2017) 1–14. doi:10.3233/ICA-170553.

[18] A. J. Nambiar, A. E. Kiprakis, D. I. M. Forehand, A. R. Wallace, Wave Energy Converter Power Take-Off Dimensioning using Particle Swarm Optimisation, IEEE Transactions on Sustainable Energy (unpublished) 1–17.

[19] R. G. Coe, G. Bacelli, D. G. Wilson, O. Abdelkhalik, U. A. Korde, R. D. Robinett III, A comparison of control strategies for wave energy converters, International Journal of Marine Energy 20 (2017) 45–63. doi:10.1016/J.IJOME.2017.11.001.

[20] J. P. Ortiz, H. Bailey, B. Buckham, C. Crawford, Surrogate Based Design of a Mooring System for a Self-reacting Point Absorber, in: Proc. of the 25th International Society of Offshore and Polar Engineers Conference (ISOPE), International Society of Offshore and Polar Engineers, 2015.

[21] J. Thomsen, F. Ferri, J. Kofoed, K. Black, J. B. Thomsen, F. Ferri, J. P. Kofoed, K. Black, Cost Optimization of Mooring Solutions for Large Floating Wave Energy Converters, Energies 11 (1) (2018) 159. doi:10.3390/en11010159.

[22] P. Mercade Ruiz, V. Nava, M. Topper, P. Minguela, F. Ferri, J. Kofoed, P. M. Ruiz, V. Nava, M. B. R. Topper, P. R. Minguela, F. Ferri, J. P. Kofoed, Layout Optimisation of Wave Energy Converter Arrays, Energies 10 (9) (2017) 1262. doi:10.3390/en10091262.

[23] F. Ferri, Computationally efficient optimisation algorithms for WECs arrays, in: Proc. of the 12th European Wave and Tidal Energy Conference (EWTEC), Cork, 2017, pp. 1–7.

[24] C. Sharp, B. DuPont, Wave energy converter array optimization: A genetic algorithm approach and minimum separation distance study,

Ocean Engineering 163 (2018) 148–156. doi:10.1016/J.OCEANENG.2018.05.071.

[25] M. Giassi, M. Göteman, S. Thomas, J. Engström, M. Eriksson, J. Isberg, Multi-Parameter Optimization of Hybrid Arrays of Point Absorber Wave Energy Converters, in: Proc. of 12th European Wave and Tidal Energy Conference (EWTEC), Cork, 2017.

[26] A. de Andres, J. Maillet, J. H. Todalshaug, P. Möller, H. Jeffrey, On the Optimum Sizing of a Real WEC from a Techno- Economic Perspective, in: Proc. of International Conference on Ocean, Offshore and Arctic Engineering (OMAE), Busan, South Korea, 2016.

[27] P. Y. Papalambros, D. J. Wilde, Principles of Optimal Design : Modeling and Computation, Cambridge University Press, 2000.

[28] E.-G. Talbi, Metaheuristcis - From design to implementation, John Wiley & Sons, 2009.

[29] E. Zitzler, M. Laumanns, S. Bleuler, A Tutorial on Evolutionary Multiobjective Optimization, in: T. V. Gandibleux X., Sevaux M., Sörensen K. (Ed.), Metaheuristics for Multiobjective Optimisation. Lecture Notes in Economics and Mathematical Systems, Springer, Berlin, Heidelberg, 2004, pp. 3–37. doi:https://doi.org/10.1007/978-3-642-17144-4_1.

[30] K. Deb, D. Kalyanmoy, Multi-objective optimization using evolutionary algorithms, John Wiley & Sons, 2001.

[31] A. F. d. O. Falcão, Wave energy utilization: A review of the technologies, Renewable and Sustainable Energy Reviews 14 (3) (2010) 899–918. doi:10.1016/j.rser.2009.11.003.

[32] I. López, J. Andreu, S. Ceballos, I. Martínez de Alegría, I. Kortabarria, Review of wave energy technologies and the necessary power-equipment, Renewable and Sustainable Energy Reviews 27 (2013) 413–434. doi:10.1016/J.RSER.2013.07.009.

[33] M. Kan, Wave-power absorption by asymmetric bodies, Tech. Rep. February, Tokyo (1979).

[34] M. Alves, A. Sarmento, Hydrodynamic Optimization of the Active surface of a Heaving Point Absorber WEC, in: Proc. of the 8th European Wave and Tidal Energy Conference (EWTEC), 2009, pp. 610–617.

[35] G. Backer, Hydrodynamic design optimization of wave energy converters consisting of heaving point absorbers, Ph.D. thesis (2009). arXiv:arXiv:1011.1669v3, doi:10.1017/CBO9781107415324.004.

[36] R. W. Yeung, Y. Jiang, Shape Effects on Viscous Damping and Motion of Heaving Cylinders, in: Proc. of the International Conference on Ocean, Offshore and Arctic Engineering (OMAE), ASME, Rotterdam, 2011. doi:10.1115/1.4027650.

[37] P. J. B. F. N. Beirão, C. M. dos Santos Pereira Malça, Design and analysis of buoy geometries for a wave energy converter, International Journal of Energy and Environmental Engineering 5 (2-3) (2014) 91. doi:10.1007/s40095-014-0091-7.
URL http://link.springer.com/10.1007/s40095-014-0091-7

[38] J. Goggins, W. Finnegan, Shape optimisation of floating wave energy converters for a specified wave energy spectrum, Renewable Energy 71 (2014) 208–220. doi:10.1016/j.renene.2014.05.022.

[39] F. Madhi, M. E. Sinclair, R. W. Yeung, The "Berkeley Wedge": an asymmetrical energy-capturing floating breakwater of high performance, Marine Systems & Ocean Technology 9 (1) (2014) 5–16.

[40] L. Sjökvist, R. Krishna, M. Rahm, V. Castellucci, A. Hagnestål, M. Leijon, On the Optimization of Point Absorber Buoys, Journal of Marine Science and Engineering 2 (2) (2014) 477–492. doi:10.3390/jmse2020477.

[41] A. de Andres, R. Guanche, C. Vidal, I. J. Losada, Adaptability of a generic wave energy converter to different climate conditions, Renewable Energy 78 (2015) 322–333. doi:10.1016/j.renene.2015.01.020.

[42] P. Garcia-Rosa, G. Bacelli, J. Ringwood, Control-Informed Geometric Optimization of Wave Energy Converters: The Impact of Device Motion and Force Constraints, Energies 8 (12) (2015) 13672–13687. doi:10.3390/en81212386.

[43] H.-J. Koh, W.-S. Ruy, I.-H. Cho, H.-M. Kweon, Multi-objective optimum design of a buoy for the resonant-type wave energy converter, Journal of Marine Science and Technology 20 (1) (2015) 53–63. doi:10.1007/s00773-014-0268-z.

[44] P. B. Garcia-Rosa, J. V. Ringwood, On the sensitivity of optimal wave energy device geometry to the energy maximizing control system, IEEE Transactions on Sustainable Energy 7 (1) (2016) 419–426. doi:10.1109/TSTE.2015.2423551.

[45] F. Kalofotias, Study for the Hull Shape of a Wave Energy Converter-Point Absorber Design Optimization & Modeling Improvement, M.sc., University of Twente (2016).

[46] D. Son, V. Belissen, R. W. Yeung, Performance validation and optimization of a dual coaxial-cylinder ocean-wave energy extractor, Renewable Energy 92 (2016) 192–201. doi:10.1016/J.RENENE.2016.01.032.

[47] W.-c. Zhang, H.-x. Liu, L. Zhang, X.-w. Zhang, Hydrodynamic analysis and shape optimization for vertical axisymmetric wave energy converters, China Ocean Engineering 30 (6) (2016) 954–966. doi:10.1007/s13344-016-0062-2.

[48] J. van Rij, Y.-H. Yu, K. Edwards, M. Mekhiche, Ocean power technology design optimization, International Journal of Marine Energy 20 (2017) 97–108. doi:10.1016/J.IJOME.2017.07.010.

[49] M. Shadman, S. F. Estefen, C. A. Rodriguez, I. C. Nogueira, A geometrical optimization method applied to a heaving point absorber wave energy converter, Renewable Energy 115 (2018) 533–546. doi:10.1016/J.RENENE.2017.08.055.

[50] S. Jin, R. J. Patton, B. Guo, Enhancement of wave energy absorption efficiency via geometry and power take-off damping tuning, Energy 169 (2019) 819–832. doi:10.1016/J.ENERGY.2018.12.074.

[51] A. Babarit, A. H. Clément, Shape optimisation of the SEAREV wave energy converter, in: Proc. of the 9th World Renewable Energy Congress, 2006.

[52] J.-C. Gilloteaux, J. Ringwood, Control-informed geometric optimisation of wave energy converters, in: Proc. of the 8th IFAC Conference on Control Applications in Marine Systems, Elsevier, 2010, pp. 366–371. doi:10.3182/20100915-3-DE-3008.00072.

[53] A. P. McCabe, G. A. Aggidis, M. B. Widden, Optimizing the shape of a surge-and-pitch wave energy collector using a genetic algorithm, Renewable Energy 35 (12) (2010) 2767–2775. doi:10.1016/j.renene.2010.04.029.

[54] A. Kurniawan, T. Moan, Multi-objective optimization of a wave energy absorber geometry, in: Proc. of the 27th International Workshop on Water Waves and Floating Bodies, no. 2, 2012, pp. 3–6.

[55] A. McCabe, Constrained optimization of the shape of a wave energy collector by genetic algorithm, Renewable Energy 51 (2013) 274–284. doi:10.1016/j.renene.2012.09.054.

[56] M. Blanco, P. Moreno-Torres, M. Lafoz, D. Ramírez, Design parameter analysis of point absorber WEC via an evolutionary-algorithm-based dimensioning tool, Energies 8 (10) (2015) 11203–11233. doi:10.3390/en81011203.

[57] O. Abdelkhalik, R. G. Coe, G. Bacelli, D. G. Wilson, WEC Geometry Optimization With Advanced Control, in: Proc. of the 36th International Conference on Ocean, Offshore and Arctic Engineering (OMAE) - Volume 10: Ocean Renewable Energy, ASME, 2017. doi:10.1115/OMAE2017-61917.

[58] M. Blanco, M. Lafoz, D. Ramirez, G. Navarro, J. Torres, L. Garcia-Tabares, Dimensioning of Point Absorbers for Wave Energy Conversion by means of Differential Evolutionary Algorithms, IEEE Transactions on Sustainable Energy (2018) 1–9doi:10.1109/TSTE.2018.2860462.

[59] A. Garcia-Teruel, D. I. M. Forehand, H. Jeffrey, Wave Energy Converter hull design for manufacturability and reduced LCOE, in: Proc. of the 7th International Conference on Ocean Energy (ICOE), 2018, pp. 1–9.

[60] A. Garcia-Teruel, D. I. M. Forehand, Optimal wave energy converter geometry for different modes of motion, in: Proc. of the 3rd International Conference on Renewable Energies Offshore (RENEW 2018) - Advances in Renewable Energies Offshore, Lisbon, 2018, pp. 299–305.

[61] A. Garcia-Teruel, D. I. M. Forehand, H. Jeffrey, Metrics for Wave Energy Converter Hull Geometry Optimisation, in: Proc. of the 13th European Wave and Tidal Energy Conference, Naples, 2019.

[62] S. A. Sirigu, L. Foglietta, G. Giorgi, M. Bonfanti, G. Cervelli, G. Bracco, G. Mattiazzo, Techno-Economic optimisation for a wave energy converter via genetic algorithm, Journal of Marine Science and Engineering 8 (8) (2020). doi:10.3390/JMSE8070482.

[63] A. Garcia-Teruel, B. DuPont, D. I. M. Forehand, Hull geometry optimisation of wave energy converters: On the choice of the optimisation algorithm and the geometry definition, Applied Energy 280 (2020). doi:10.1016/j.apenergy.2020.115952.

[64] R. Guanche, V. Gómez, C. Vidal, I. Eguinoa, Numerical analysis and performance optimization of a submerged wave energy point absorber, Ocean Engineering 59 (2013) 214–230. doi:10.1016/J.OCEANENG.2012.10.016.

[65] S. Crowley, R. Porter, D. V. Evans, A submerged cylinder wave energy converter, Journal of Fluid Mechanics 716 (2013) 566–596. doi:10.1017/jfm.2012.557.

[66] A. Kurniawan, J. R. Chaplin, D. M. Greaves, M. Hann, Wave energy absorption by a floating air bag, Journal of Fluid Mechanics 812 (2017) 294–320. doi:10.1017/jfm.2016.811.

[67] G. P. Thomas, B. P. Gallagher, An assessment of design parameters for the Bristol cylinder, in: Proc. of the European Wave Energy Symposium, no. 1981, 1993, pp. 139–144.

[68] S. H. Crowley, R. Porter, D. V. Evans, A submerged cylinder wave energy converter with internal sloshing power take off, European Journal of Mechanics, B/Fluids 47 (2014) 108–123. doi:10.1016/j.euromechflu.2014.03.008.

[69] S. Esmaeilzadeh, M. R. Alam, Shape optimization of wave energy converters for broadband directional incident waves, Ocean Engineering 174 (2019) 186–200. arXiv:1805.08294, doi:10.1016/j.oceaneng.2019.01.029.

[70] S. A. Mavrakos, G. M. Katsaounis, M. S. Apostolidis, Effect of Floaters' Geometry on the Performance Characteristics of Tightly Moored Wave Energy Converters, in: Proc. of the 28th International Conference on Ocean, Offshore and Arctic Engineering (OMAE), ASME, Honolulu, 2009, pp. 1145–1152. doi:10.1115/OMAE2009-80133.

[71] S. J. Beatty, M. Hall, B. J. Buckham, P. Wild, B. Bocking, Experimental and numerical comparisons of self-reacting point absorber wave energy converters in regular waves, Ocean Engineering 104 (2015) 370–386. doi:10.1016/j.oceaneng.2015.05.027.

[72] A. Kurniawan, M. Grassow, F. Ferri, Numerical modelling and wave tank testing of a self-reacting two-body wave energy device, Ships and Offshore Structures 14 (sup1) (2019) 344–356. doi:10.1080/17445302.2019.1595924.

[73] R. Gomes, J. C. C. Henriques, L. M. C. Gato, A. F. O. Falcão, IPS Two-body Wave Energy Converter : Acceleration Tube Optimization, in: Proc. of the International Society of Offshore and Polar Engineers Conference (ISOPE), Vol. 7, 2010, pp. 834–842. doi:10.13140/2.1.2805.6321.

[74] M. Blanco, M. Lafoz, G. Navarro, Wave energy converter dimensioning constrained by location, power take-off and control strategy, in: Proc. of 2012 IEEE International Symposium on Industrial Electronics, IEEE, 2012, pp. 1462–1467. doi:10.1109/ISIE.2012.6237307.

[75] V. Neary, R. Coe, J. Cruz, K. Haas, G. Bacelli, Y. Debruyne, S. Ahn, V. Nevarez, Classification Systems for Wave Energy Resources and WEC Technologies, in: Proc. of the 12th European Wave and Tidal Energy Conference (EWTEC), no. Iii, 2017, pp. 973–1—-973–9.

[76] Y.-H. Yu, Y. Li, K. Hallet, C. Hotismky, Design and Analysis for a Floating Oscillating Surge Wave Energy Converter, in: Proc. of 33rd

International Conference on Ocean, Offshore and Arctic Engineering (OMAE), San Francisco, CA, 2014.

[77] N. Tom, A. Wright, M. Lawson, Y.-h. Yu, Preliminary Analysis of an Oscillating Surge Wave Energy Converter with Controlled Geometry, in: European Wave and Tidal Energy Conference, 2015, pp. 1–10.

[78] A. Kurniawan, T. Moan, Optimal geometries for wave absorbers oscillating about a fixed axis, IEEE Journal of Oceanic Engineering 38 (1) (2013) 117–130. doi:10.1109/JOE.2012.2208666.

[79] I. F. Noad, R. Porter, Optimisation of arrays of flap-type oscillating wave surge converters, Applied Ocean Research 50 (2015) 237–253. doi:10.1016/j.apor.2015.01.020.

[80] E. Renzi, J. Leech, I. Phillips, WEC-GA optimisation tool for an oscillating wave surge converter, in: Proc. of the 12th European Wave and Tidal Energy Conference (EWTEC), 2017, pp. 874.1–874.6.

[81] C. Anderson, Pelamis WEC Main Body Structural Design And Materials Selection, Tech. rep., Ocean Power Delivery Ltd. (2003).

[82] H. R. Le, K. M. Collins, D. M. Greaves, N. W. Bellamy, Mechanics and materials in the design of a buckling diaphragm wave energy converter, Materials and Design 79 (2015) 86–93. doi:10.1016/j.matdes.2015.04.041.

[83] I. F. Noad, R. Porter, Modelling an articulated raft wave energy converter, Renewable Energy 114 (2017) 1146–1159. doi:10.1016/j.renene.2017.07.077.

[84] P. Haren, C. C. Mei, Wave power extraction by a train of rafts: hydrodynamic theory and optimum design, Applied Ocean Research 1 (3) (1979) 147–157. doi:10.1016/0141-1187(79)90014-2.

[85] M. Colby, E. Nasroullahi, K. Tumer, Optimizing Ballast Design of Wave Energy Converters Using Evolutionary Algorithms, in: Proc. of the 13th Annual Conference on Genetic and Evolutionary Computation, 2011, pp. 1739–1746.

[86] R. Costello, B. Teillant, J. Weber, J. V. Ringwood, Techno-Economic Optimisation for Wave Energy Converters, in: Proc. of the 4h International Conference on Ocean Energy (ICOE), 2012.

[87] T. J. Whittaker, F. A. Mc Peake, A. G. Barr, The development and testing of a wave-activated navigation buoy with a wells turbine, Journal of Energy Resources Technology, Transactions of the ASME 107 (2) (1985) 268–273. doi:10.1115/1.3231188.

[88] A. F. Falcão, J. C. Henriques, J. J. Cândido, Dynamics and optimization of the OWC spar buoy wave energy converter, Renewable Energy 48 (2012) 369–381. doi:10.1016/J.RENENE.2012.05.009.

[89] F. Mahnamfar, A. Altunkaynak, Comparison of numerical and experimental analyses for optimizing the geometry of OWC systems, Ocean Engineering 130 (November 2015) (2017) 10–24. doi:10.1016/j.oceaneng.2016.11.054.

[90] G. Palma, S. Mizar Formentin, B. Zanuttigh, P. Contestabile, D. Vicinanza, Numerical Simulations of the Hydraulic Performance of a Breakwater-Integrated Overtopping Wave Energy Converter, Journal of Marine Science and Engineering 7 (2) (2019) 38. doi:10.3390/jmse7020038.

[91] D. V. Evans, B. P. O'Gallachoir, R. Porter, G. P. Thomas, On the optimal design of an oscillating water column device, in: Proc. of the 2nd European Wave Energy Conference (EWTEC), 1995, pp. 172–178.

[92] J. Weber, G. P. Thomas, Optimisation of the hydro-aerodynamic coupling of a 2-d onshore and a 3-dnearshore Oscillating Water Column wave energy device, in: Proc. of MAREC 01, Newcastle, England, 2000, pp. 193–205.

[93] J. Weber, G. P. Thomas, Some aspects of the design optimisation of an OWC with regard to multiple sea states and combined object functions, in: Proc. of the 5th European Wave Energy Conference (EWTEC), 2003, pp. 141–148.

[94] J. Weber, G. P. Thomas, Optimisation of the Hydrodynamic-Aerodynamic Coupling of an Oscillating Water Column Wave Energy

Converter Wave Energy Device, in: Proc. of the 4th European Wave Energy Conference (EWTEC), 2001, pp. 251–259.

[95] J. Weber, G. P. Thomas, Turbine type & design selection in the context of multi-parametric overall system optimisation of Oscillating Water Column wave energy converters Introduction & Motivation, in: Proc. of the International Conference on Ocean Energy (ICOE), Bremerhaven, Germany, 2006.

[96] R. Gomes, J. Henriques, L. Gato, A. Falcão, Hydrodynamic optimization of an axisymmetric floating oscillating water column for wave energy conversion, Renewable Energy 44 (2012) 328–339. doi:10.1016/J.RENENE.2012.01.105.

[97] S. Ribeiro E Silva, R. P. Gomes, A. F. Falcaõ, Hydrodynamic optimization of the UGEN: Wave energy converter with U-shaped interior oscillating water column, International Journal of Marine Energy 15 (2016) 112–126. doi:10.1016/j.ijome.2016.04.013.

[98] T. K. Das, P. Halder, A. Samad, Optimal design of air turbines for oscillating water column wave energy systems: A review, The International Journal of Ocean and Climate Systems 8 (1) (2017) 37–49. doi:10.1177/1759313117693639.

[99] S. Mishra, S. Purwar, N. Kishor, Maximizing Output Power in Oscillating Water Column Wave Power Plants: An Optimization Based MPPT Algorithm, Technologies 6 (1) (2018) 15. doi:10.3390/technologies6010015.

[100] A. de Andres, J. Maillet, J. Hals Todalshaug, P. Möller, D. Bould, H. Jeffrey, Techno-Economic Related Metrics for a Wave Energy Converters Feasibility Assessment, Sustainability 8 (11) (2016) 1109. doi:10.3390/su8111109.

[101] S. Astariz, G. Iglesias, The economics of wave energy: A review, Renewable and Sustainable Energy Reviews 45 (2015) 397–408. doi:10.1016/j.rser.2015.01.061.

[102] A. Babarit, J. Hals, M. Muliawan, A. Kurniawan, T. Moan, J. Krokstad, Numerical benchmarking study of a selection of wave en-

ergy converters, Renewable Energy 41 (2012) 44–63. doi:10.1016/j.renene.2011.10.002.

[103] J. Weber, R. Costello, J. Ringwood, WEC technology performance levels (TPLs)- metric for successful development of economic WEC technology., in: Proc. of 10th European Wave and Tidal Energy Conference (EWTEC), EWTEC, 2013.

[104] H. Eidsmoen, Tight-moored amplitude-limited heaving-buoy wave-energy converter with phase control, Applied Ocean Research 20 (3) (1998) 157–161. doi:10.1016/S0141-1187(98)00013-3.

[105] W. Cummins, The impulse response function and ship motions, Tech. rep., Department of the Navy, David Taylor model basin (1962).

[106] R. Taghipour, T. Perez, T. Moan, Hybrid frequency–time domain models for dynamic response analysis of marine structures, Ocean Engineering 35 (7) (2008) 685–705. doi:10.1016/J.OCEANENG.2007.11.002.

[107] D. V. Evans, R. Porter, Wave energy extraction by coupled resonant absorbers, Philosophical Transactions of the Royal Society A: Mathematical, Physical and Engineering Sciences 370 (1959) (2012) 315–344. doi:10.1098/rsta.2011.0165.

[108] D. V. Evans, R. Porter, Hydrodynamic characteristics of an oscillating water column device, Applied Ocean Research 17 (3) (1995) 155–164. doi:10.1016/0141-1187(95)00008-9.

[109] A. Babarit, A database of capture width ratio of wave energy converters, Renewable Energy 80 (2015) 610–628. doi:10.1016/j.renene.2015.02.049.

[110] D. V. Evans, A theory for wave-power absorption by oscillating bodies, Journal of Fluid Mechanics 77 (1) (1976) 1–25. doi:10.1017/S0022112076001109.

[111] J. Falnes, Ocean Waves and Oscillating Systems, Cambridge University Press, New York, 2002.

[112] C. E. Clark, A. Garcia-Teruel, B. DuPont, D. I. M. Forehand, Towards reliability-based geometry optimization of a point-absorber with

PTO reliability objectives, in: Proc. of 13th European Wave and Tidal Energy Conference (EWTEC), Naples, 2019.

[113] Y.-H. Yu, J. Van Rij, R. Coe, M. Lawson, Preliminary Wave Energy Converters Extreme Load Analysis, in: Proc. of the 34th International Conference on Ocean, Offshore and Arctic Engineering (OMAE), ASME, St. John's, Newfoundland, Canada, 2015. doi:10.1115/OMAE2015-41532.

[114] J. van Rij, Y.-H. Yu, Y. Guo, Structural Loads Analysis for Wave Energy Converters, in: Proc. of the 36th International Conference on Ocean, Offshore and Arctic Engineering (OMAE), ASME, Trondheim, Norway, 2017. doi:10.1115/OMAE2017-62139.

[115] J. van Rij, Y.-H. Yu, R. G. Coe, Design Load Analysis for Wave Energy Converters, in: Proc. of the 37th International Conference on Ocean, Offshore and Arctic Engineering (OMAE), ASME, Madrid, Spain, 2018. doi:10.1115/OMAE2018-78178.

[116] Wave Energy Scotland, Structural Forces and Stresses for Wave Energy Devices Final Report WES_LS02_ER_Forces and Stresses Structural Forces and Stresses for Wave Energy Devices - Landscaping Study (2016).

[117] R. G. Coe, Y.-H. Yu, J. van Rij, A Survey of WEC Reliability, Survival and Design Practices, Energies 11 (1) (2017) 4. doi:10.3390/en11010004.

[118] R. G. Coe, C. Michelen, A. Eckert-Gallup, Y.-H. Yu, J. van Rij, WDRT: A toolbox for design-response analysis of wave energy converters, Proc. of the 4th Marine Energy Technology Symposium (2016).

[119] J. H. Holland, Adaptation in natural and artificial systems : an introductory analysis with applications to biology, control, and artificial intelligence, University of Michigan Press, Ann Arbor, 1975.

[120] E. Renzi, F. Dias, Resonant behaviour of an oscillating wave energy converter in a channel, Journal of Fluid Mechanics 701 (2012) 482–510. doi:10.1017/jfm.2012.194.

[121] ESTECO, modeFrontier — www.esteco.com.
URL https://www.esteco.com/modefrontier

[122] A. Babarit, G. Delhommeau, Theoretical and numerical aspects of the open source BEM solver NEMOH., in: In Proc. of the 11th European Wave and Tidal Energy Conference (EWTEC2015), Nantes, France, 2015.

[123] MIT, WAMIT User Manual (2016).
URL http://www.wamit.com/manualupdate/V70{_}manual.pdf

[124] ANSYS Inc., Ansys Aqwa: Hydrodynamics Simulation & Diffraction Analysis — Ansys.
URL https://www.ansys.com/products/structures/ansys-aqwa

[125] K. Ruehl, C. Michelen, S. Kanner, M. Lawson, Y.-H. Yu, Preliminary verification and validation of WEC-Sim, an open-source wave energy converter design tool, in: Proc. of the 33rd International Conference on Ocean, Offshore and Arctic (OMAE), San Francisco, CA, 2014, pp. 1–7.

[126] Y.-H. Yu, M. Lawson, K. Ruehl, C. Michelen, Development and Demonstration of the WEC-Sim Wave Energy Converter Simulation Tool, in: Proc. of the 2nd Marine Energy Technology Symposium (METS2014), Seattle, WA, 2014, pp. 1–8.

[127] J. van Rij, Y. H. Yu, Y. Guo, R. G. Coe, A wave energy converter design load case study, Journal of Marine Science and Engineering 7 (8) (2019) 1–22. doi:10.3390/jmse7080250.

[128] NREL, Sandia, WEC-Sim (Wave Energy Converter SIMulator) — WEC-Sim documentation.
URL https://wec-sim.github.io/WEC-Sim/

[129] D. Bull, A. Dallman, Wave Energy Prize experimental sea state selection, in: Proc. of the 36th International Conference on Ocean, Offshore & Arctic Engineering (OMAE), Trondheim, 2017.

[130] W. J. Roux, N. Stander, R. T. Haftka, Response surface approximations for structural optimization, International Journal for Numerical

Methods in Engineering 42 (3) (1998) 517–534. doi:10.1002/(SICI)1097-0207(19980615)42:3<517::AID-NME370>3.0.CO;2-L.

[131] F. Driscoll, J. Weber, S. Jenne, R. Thresher, L. J. Fingersh, D. Bull, A. Dallman, B. Gunawan, A. Labonte, D. Karwat, S. Beatty, Methodology to Calculate the ACE and HPQ Metrics Used in the Wave Energy Prize (March 2018) (2018).